

Electronic Theses and Dissertations, 2004-2019

2015

Spray Deposition Modeling of Carbon Nano-Inks

John Sparkman
University of Central Florida

 Part of the [Mechanical Engineering Commons](#)
Find similar works at: <https://stars.library.ucf.edu/etd>
University of Central Florida Libraries <http://library.ucf.edu>

This Masters Thesis (Open Access) is brought to you for free and open access by STARS. It has been accepted for inclusion in Electronic Theses and Dissertations, 2004-2019 by an authorized administrator of STARS. For more information, please contact STARS@ucf.edu.

STARS Citation

Sparkman, John, "Spray Deposition Modeling of Carbon Nano-Inks" (2015). *Electronic Theses and Dissertations, 2004-2019*. 5033.
<https://stars.library.ucf.edu/etd/5033>

SPRAY DEPOSITION MODELING OF CARBON NANO-INKS

by

JOHN SPARKMAN
B.S. University of Central Florida, 2013

A thesis submitted in partial fulfillment of the requirements
for the degree of Master of Science
in the Department of Mechanical and Aerospace Engineering
in the College of Engineering and Computer Science
at the University of Central Florida
Orlando, Florida

Summer Term
2015

Major Professor: Jihua Gou

ABSTRACT

Carbon nanopaper (CNP) exhibits qualities that are desirable for a number of applications such as flame retardancy, lightning protection, and flexible printed circuit boards. CNP has become a desired engineering material in many important sectors of industries such as space, automotive, aviation, and military. However the production of consistent thicknesses and dispersion remains a challenge for practical use. Most of the standard methods of production do not allow for continuous applications or digital fabrication of the CNP.

In this work, CNP is produced two different ways that allows for continuous production and digital fabrication. The continuous CNP making technique uses vacuum infiltration along with air atomization and a continuous drive belt system to produce a continuous roll of the CNP. This system is able to produce an $11 \mu\text{m} \pm 2 \mu\text{m}$ CNP at 6 inches per min with an electrical resistivity of 59Ω per square. The major advantage of this production process is the ability to mass manufacture the CNP. Spray deposition modeling (SDM) is a digital fabrication process that uses a 12 array bubble jet nozzle attached to a digital control x-y plotter combined with a heated substrate which induces evaporation. This process is able to produce paper with variable thicknesses in defined locations. The maximum thickness of the CNP produced is $10 \mu\text{m}$ with a resistivity of 95.7Ω per square. A strong advantage of this CNP production method comes from the ability to digitally print images. The controllable thickness and selective location printing presents an effective alternative to costlier methods and provides a solution to many geometrical CNP issues.

ACKNOWLEDGMENTS

I would first like to thank Dr. Jihua Gou for giving me the opportunity to continue my education and providing me with the materials and support to understand composites materials. His guidance over the past two years has provided me with the knowledge and abilities to continue working in the field of composites, and strive for innovating and creating machinery for the future of composites.

I would also like to thank my thesis committee members, Dr. Yunjun Xu and Dr. Kurt Lin for their interest in my research and taking the time to review and evaluate my thesis. Another person who deserves acknowledgment for their contribution for earlier works and guidance is Dr. Fei Liang.

Some of my experiments that were needed could not have been done without the help of one of my co-worker Xin Wang and her experience with the scanning electron microscopy. The SEM machine that was used was at the material facility characterization center.

I would also like to give special thanks to the senior design team who originally designed the machine that my thesis is based on. Their work over two semesters provided me with a moderately working machine that needed little work to provide data for my experiments.

Finally, I would like to thank my wife Chie Sparkman who has supported me through my entire college career. I could not have done it without her help and support.

TABLE OF CONTENTS

ABSTRACT.....	ii
ACKNOWLEDGMENTS	iii
TABLE OF CONTENTS.....	iv
LIST OF FIGURES	vii
LIST OF TABLES.....	ix
CHAPTER ONE: INTRODUCTION.....	1
1.1 Motivation.....	1
1.2 Research on Continuous Deposition of Nanoparticles.....	3
1.3 Research on Spray Deposition Modeling.....	3
1.4 Objectives.....	5
1.5 Thesis Outline	5
CHAPTER TWO: LITERATURE REVIEW.....	7
2.1 Carbon Nanotubes	7
2.2 Carbon Nanopaper.....	8
2.3 Digital Fabrication Techniques of CNT-Inks.....	12
CHAPTER THREE: METHODOLOGY	15
3.1 Introduction	15
3.2 Preparation of the CNT-Inks and SMP Resin	17
3.3 Spray Infiltration Method.....	18
3.3.1 Spraying Method.....	19
3.3.2 Fabrication Process	20
3.3.3 Processing Effects.....	22

3.4 Spray Deposition Modeling	23
3.4.1 Spraying Method.....	23
3.4.2 Fabrication Process	24
3.4.3 Controls.....	26
3.4.4 Processing Effects	27
3.5 Resin Deposition Method.....	28
3.5.1 Film Fabrication.....	28
3.5.2 Processing Effects	31
CHAPTER FOUR: TESTING AND EVALUATION	32
4.1 Introduction	32
4.2 Spray Infiltration Method.....	34
4.2.1 Electrical Resistivity	34
4.2.2 Thermal Testing.....	36
4.2.3 Thickness Measurements	39
4.2.4 Weight Measurements	42
4.3 Spray Deposition Modeling	43
4.3.1 Electrical Resistivity	43
4.3.2 Thermal Testing.....	45
4.3.3 Weight Measurements	48
4.3.4 Actuation.....	50
4.4 Comparing SDM to Current Methods.....	51
CHAPTER FIVE: CONCLUSION AND FUTURE WORK.....	53
5.1 Concluding the Spray Infiltration Process	53

5.2 Concluding Spray Deposition Modeling.....	54
5.3 Future Work	55
APPENDIX A: CNC CODE.....	57
A.1 G-Code	58
A.2 M-Code.....	58
A.3 A-Code	60
APPENDIX B: MATLAB CODE	62
APPENDIX C: PROCESSING CODE.....	66
LIST OF REFERENCES.....	70

LIST OF FIGURES

Figure 1 Schematic of Vacuum Infiltration Method.....	9
Figure 2 Schematic of Pressure Filtration Method	10
Figure 3 Schematic of Frit Compression Method.....	11
Figure 4 Schematic of Domino Pushing Method.....	11
Figure 5 Ink-Jet Processes a) Thermal Jet b) Piezo Jet.....	12
Figure 6 Sheet Resistance Versus Number of Prints [25].....	14
Figure 7 Types of Spray Patterns.....	16
Figure 8 Digital Composite Manufacturing.....	17
Figure 9 Pneumatic Spray Distribution Schematic.....	19
Figure 10 Spray Infiltration Fabrication Process	20
Figure 11 Samples Produced by Spray Infiltration Method	21
Figure 12 Processing Effects of Spray Infiltration using Cellulose Filter Paper	22
Figure 13 Spray Deposition Modeling's Spraying Method	24
Figure 14 SDM Fabrication Process	25
Figure 15 Samples Produced by SDM Process.....	25
Figure 16 G-Code Processing in Matlab a) Nozzle Travel b) Droplet Pattern for 3 Nozzles	27
Figure 17 a) Black and White image of the Model b) the printed model	27
Figure 18 Film Fabrication of Spray Infiltrated CNP	29
Figure 19 Film Fabrication of Spray Infiltration CNP	30
Figure 20 Film Fabrication of SDM	30
Figure 21 Processing Effects of Depositing Resin	31
Figure 22 Schematic of the Four Point Probe test for Resistivity Measurements	33

Figure 23 Electrical Resistivity Measurements for Spray Infiltration Method.....	34
Figure 24 Resistivity Measurements over the Area	35
Figure 25 Thermal Image of the Spray Infiltration Sample.....	37
Figure 26 Temperature vs. Current Measurements for Spray Infiltration Method.....	38
Figure 27 Cross Section SEM Image of the 100 μm CNP	40
Figure 28 Thickness vs. Speed Chart for the Spray Infiltration Method	41
Figure 29 Weight vs. Speed Measurements for the Spray Infiltration Method	42
Figure 30 Weight vs. Volume Measurements for the Spray Infiltration Method.....	43
Figure 31 Electrical Resistivity Measurements from Layering	44
Figure 32 Electrical Resistivity of each Layer over the Distance for SDM	45
Figure 33 Thermal Heating of the SMP Thin Film using SDM Processing.....	46
Figure 34 Temperature vs. Voltage Graph for SDM	47
Figure 35 Lowering the Weight by Lowering the Feed Rate in SDM.....	49
Figure 36 Increasing the Weight by Layering Using SDM	50
Figure 37 Actuation of the SDM Sample	51

LIST OF TABLES

Table 1 Resistivity Measurements for Spray Infiltration Method	36
Table 2 Thermal Measurements for the Spray Infiltration Method	39
Table 3 Thickness Measurements for the Spray Infiltration Method	41
Table 4 Temperature, Voltage, and Current Measurements for SDM.....	48

CHAPTER ONE: INTRODUCTION

1.1 Motivation

A composite material is the combination of two or more materials that have either physical or chemical differences, and when combined produce characteristics that differ from the individual components. So, a composite is not only made from plastics, but can be made from any material that is able to be combined together, this includes but is not limited to metals, woods, thermosets, and thermoplastics. Plastic composites have two different parts that make it a composite. The filler material and the binder, the binder is usually made of a thermoset. A thermoset can be a one or two part epoxy that cures with temperature, but is not able to be reused. This non-reusability material makes it noxious to the environment, so it would be more acceptable to use reusable materials. Some research is being done on the removal of fibers from a thermoset, but most of the time they are damaged upon removal. Fibers used in composites can have different orientations and be used in different ways. For example there are random oriented fibers in the composite, or the fibers can be made into fabric or thread. All the ways fibers are added to the composite to form the matrix gives it different properties and characteristics. The fabrics made from the fiber can also have different forms such as plain, basket, or twill this also has some property effects on the overlying matrix.

Composites started thousands of years ago mainly to construct buildings. Now composites are used in everything from cars to aircrafts. Placing composites in such machines started in the mid 70's and is used more today than then. It is projected by the year 2016 the composites industry will become a 16 billion dollar industry and continue to grow. Composites make machines lighter in weight, which in aircrafts and cars, means better fuel efficiency. The

new Boeing 787 has over 50% of the entire aircraft made of composite materials. It has been more recently that composites have been used more in industry; prior to this it was mainly used for military applications. As of now, the manufacturing of composites has been highly sought after to better enhance the workings and usage of composites. The reason for the industries growth is a better understanding of how to produce the materials; and with the enhancement of computers, the knowledge of how the materials work and react is much better.

One of the most difficult parts of a composite is the inability to mass manufacture, in contrast to metals. Composites are able to be manufactured in many different ways; depending on the application needed. Some ways to make composites are by doing a hand layup process, extrusion, vacuum assisted resin transfer molding (VARTM), and resin transfer molding (RTM). A hand layup process is done using a human to deposit each layer of material individually, then smooth or roll out the excess air inside of the material. Extrusion is the pushing of the fibers and the resin through a mold. Extrusions can also have holes in the part. VARTM is another form of manufacturing that is used with or without an autoclave assist, in which the resin is pulled with a vacuum to infiltrate the fibers. RTM is similar to VARTM but instead of using vacuum it uses pressure in infiltrate the fibers. This is widely used with large pieces, like wind turbine blades.

After analyzing many of the options for manufacturing composites there seem to be a border dividing humans and machines. Most composite work is done by humans, but one way that has not been used or sought after yet, is printing the fibers into the bonder and using machines to accomplish this. The development of a machine that has the ability to deposit the matrix materials onto a substrate, without the use of vacuum or pressure, and allowing the bonder to penetrate the matrix would be a very useful machine.

1.2 Research on Continuous Deposition of Nanoparticles

Continuous nanoparticle deposition using vacuum filtration is used to produce high quality nanopaper that is able to be used in multiple applications. This type of machine uses a hydrophobic porous substrate, such as cellulose, to allow for easy removal of the solvent. This removal allows for the nanoparticles to remain on top of the substrate to produce the ending nanopaper. The solution for this process uses solvent, dispersant, and the nanoparticles. In this research the nanoparticles used are carbon nanotubes (CNTs), carbon nanofibers (CNFs), and Graphene flakes. After the materials were combined sonication was used to deagglomerate the nanoparticles and allow for better atomization of the spray and higher quality of nanopaper production.

This type of machine is able to be used in large scale applications, which is great for mass manufacturing. After manufacturing the paper, a polyurethane material could be applied to the underside of the paper to dissolve the cellulous and create a nanoparticle polyurethane film. This film could then be used to electrically actuate shape memory polymer (SMP) by using resistive heating with the CNF and the CNT.

1.3 Research on Spray Deposition Modeling

Spray Deposition Modeling (SDM) is a highly sought after method due to its ability to deposit nano-materials onto a substrate without having to use a primary method of delivery. In most cases, the nano-materials would be placed onto a porous substrate then transferred to the ending part like the continuous deposition mentioned above, but in SDM there is no need for a porous substrate or transfer because the materials are delivered onto the objective substrate directly. One of the main uses for SDM is to create composites with functional electrical

properties, but SDM is also able to enhance mechanical, electrical, and thermal properties in composites as well.

The research that was conducted for SDM shows the ability to apply multiple types of nanoparticles onto an array of substrates without the use of a porous substrate. Some of the substrates that were used were Aluminum foil, Aluminum plate, SMP, Teflon, and Copper sheeting. The materials that were used were CNTs, heliacal carbon nanotubes (HCTNs), CNFs, and Graphene flakes. They were first placed into a suspension before being sprayed onto the substrates directly.

There were two different types of suspensions used for SDM processing; one was water and the other was Ethanol. These suspensions, along with some dispersant were used in order to deagglomerate the nanoparticles to enhance their spraying ability. The process that excites deagglomeration is the introduction of sonication. Sonication is the conversion of electrical signal into a vibration. This vibration, along with the dispersant, is what causes the nanoparticles to disperse in the solution and prevent clogging the SDM machine.

The nanoparticles that were chosen for this research all have enhanced electrical properties. This electrical enhancement is great for creating flexible printed circuit boards (PCBs), or sensors. One aspect of this research is to encompass this with SMP to allow for distributed electrical resistive heating for shape actuation of the SMP. Some of the SMP thin films that were manufactured are thinner than 20 μm . The process to manufacture the SMP thin film consists of spraying a solution of SMP, which has been diluted in dimethylformamide (DMF), onto an aluminum substrate. Then SDM is used to apply the nano-ink solution and then another coating of SMP is applied. This traps the nano-ink into the SMP to allow for better heat transfer.

1.4 Objectives

The objective of this study is to develop machines that are able to produce CNP using two different process, continuous and batch. Continuous processing of CNP is done using vacuum assisted infiltration to help build the nano materials to form a thin sheet of CNP. The batch process is a digital fabrication process that uses evaporative techniques to disperse the nanomaterials in a defined location. The major focuses for the continuous process is the ability to produce continuous samples, enhance the manufacturing process by improving the quality of the CNP, and improve the production rate of the manufactured CNP. While the major focus for the batch process is to develop a digital fabrication for the development of CNP, produce high quality samples, enhance the printing process with the current CNT-inks, and print a heating element to distribute the heat on shape memory polymer (SMP) film. Both of these machines will be characterized by determining the electrical resistivity of the produced films, determining the heat produced with the addition of voltage, enhancement of the rate of production, and finding a trend of weight to dispersed material.

1.5 Thesis Outline

This thesis will start with chapter two, which will give a brief overview of the continuous fabrication of the nanopaper and how it has evolved. SDM will be further elaborated upon in more detail, while highlighting its differences from other processes on the market today. Chapter three will discuss the processing methods of some nanomaterials and the solvents used for both the continuous fabrication and the SDM process. It will also describe, in detail, the thermoplastic films process and the characterization of their electrical properties. In addition, the coding behind the machines and how that is incorporated in the processing, development, and quality control of

the products. Chapter four discusses the analysis of the machines and how they are characterized. Finally, this thesis will conclude on all of the findings gathered in Chapter 5.

CHAPTER TWO: LITERATURE REVIEW

2.1 Carbon Nanotubes

Nano-materials have been widely mentioned in recent years because of their amazing properties, and their ability to be added into coatings to improve the functionality. Some types of nano-materials used in spray applications include nano-fibers, nano-tubes, Graphene flakes, and carbon black. The potential for nano-composites reinforced with carbon tubes having extraordinary specific stiffness and strength represent tremendous opportunity for application in the 21st century [1]. These materials are not the only ones that are able to be used in spray applications, but for this paper these will be the main ones discussed. Using these types of nano-materials in composites allows for a multitude of functionalities, some examples include higher electrical and thermal conductivity, increased Young's modulus, and an increase in strength. In some instances these functions are needed more than others, to make PCB's that are flexible and that have a high electrical conductivity these types of nano-composites are needed.

A single walled carbon nanotube is able to be described as a graphene sheet that has been rolled to form a CNT [2]. This structure has several variations and is able to provide different properties. Studies done by Wildoer et al. [3] and Odom et al [4] suggest that these structures provide different electrical behaviors. One of the lowest resistivity's found for CNTs is $10^{-4} \Omega \cdot m$ [5]. This value was also found by other researches as well. Another group found that this resistivity also varied when introduced to other temperatures. Song et al. [6] found these values to be 0.65×10^{-4} at 300 K and 1.6×10^{-4} at 5 K. Using non-contact AMF a lower resistivity can be found. Issi et al. [7] found at room temperature of 300 K a resistivity of $9.5 \times 10^{-5} \Omega \cdot m$. His

worked was compared to Langer et al. [8] and he found a consistency with the measurement. The range of resistivity for Langer et al. [8] is between 10^{-4} and $10^{-5} \Omega \cdot m$.

Thermally CNTs have great stability and can be used in various applications to encourage thermal distribution and dispersion. Hone [9] found that the conductivity of CNTs were different for SWCNT and MWCNTs. The SWCNT has a thermal conductivity of $200 \text{ W/m} \cdot \text{K}$ while MWCNTs have a conductivity of $3000 \text{ W/m} \cdot \text{K}$; these values were found at room temperature. Just like the electrical properties of CNTs the thermal properties also depend on temperature, which was found by Berber et al. [10]. CNTs can also be used with other materials to enhance their thermal conductivity properties as well. Hone et al. [11] found a 120% increase in conductivity with the addition of 1 wt % of CNT.

Carbon Nano-Tubes are on the leading front of innovation; these materials are being used in all applications from synthetic muscles, flexible PCB's, and electrically conductive filament. This material not only has amazing electrical conductivity it also has great mechanical properties as well. Some of these properties include a tensile strength of 11-63 GPa, bending strength of 28.5 GPa, and a Young's Modulus of 270-950 GPa [12]. All of these values also depend on what type of CNT was used and what the precursor was that made these CNT's. For the values shown above the CNT's are multi-walled CNT's and the precursor is carbon-carbon, if Si-C was used the bending strength would have been increased to 54.2 GPa [12].

2.2 Carbon Nanopaper

Traditionally carbon composites were made by placing the carbon materials directly into the polymer matrix. However, CNTs have a strong tendency to aggregate due to their long aspect ratio and strong Van der Waals force. Some composites have seen a CNT volume fraction of up to 17% [13]. With the addition of CNTs an increase in Young's Modulus as high as 20% [14].

But due to the effects of agglomeration and the low amount of CNTs in the matrix, CNP is production widely sought after. Dispersing the CNTs into a solution is done in several ways the most common way is by using ultrasonication. Ultrasonication is an effective method to disperse CNTs in liquids having a low viscosity [15]. Dispersion of the nanotubes using the sonication process is done with the addition of a dispersant [16]. This method can be used with SWCNTs and MWCNTs to deagglomerate them.

Carbon nanopaper is a thin sheet of layered carbon nanotubes that are randomly arrayed. The first production of CNP started with porous paper, a funnel, and a vacuum Figure 1 [17]. The method was to attach the vacuum line to the small end of the funnel and place the filter paper at the top, and while the vacuum was pulling from underneath the carbon nanotube solution was poured onto the filter paper. This allowed the solvent to pulled through while leaving the CNTs behind, creating the first CNP or “bucky paper”. This method is regarded as a simple process for the fabrication of ultrathin, transparent, optically homogeneous, electrically conducting coating films composed of pure single-walled CNTs [18].

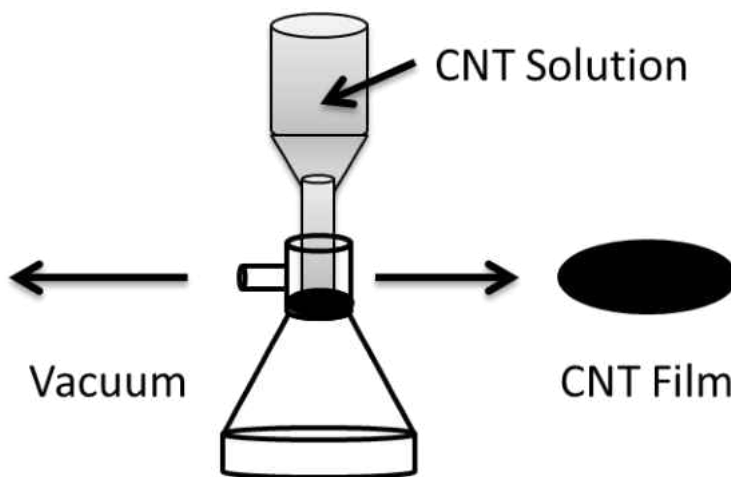


Figure 1 Schematic of Vacuum Infiltration Method

Another alternative to vacuum infiltration is pressure filtration Figure 2. In this method the porous filter paper is placed in the bottom of a pressure pot covering the exit of the chamber, while the solution sits on the top of the substrate. The pot is sealed then air pressure is applied to the top; which forces the material and solution down to the exit spout at the bottom. Since the filter paper is porous the solvent is able to escape leaving behind tightly packed CNP. This method is able to produce thicker CNP than with the vacuum infiltration method.

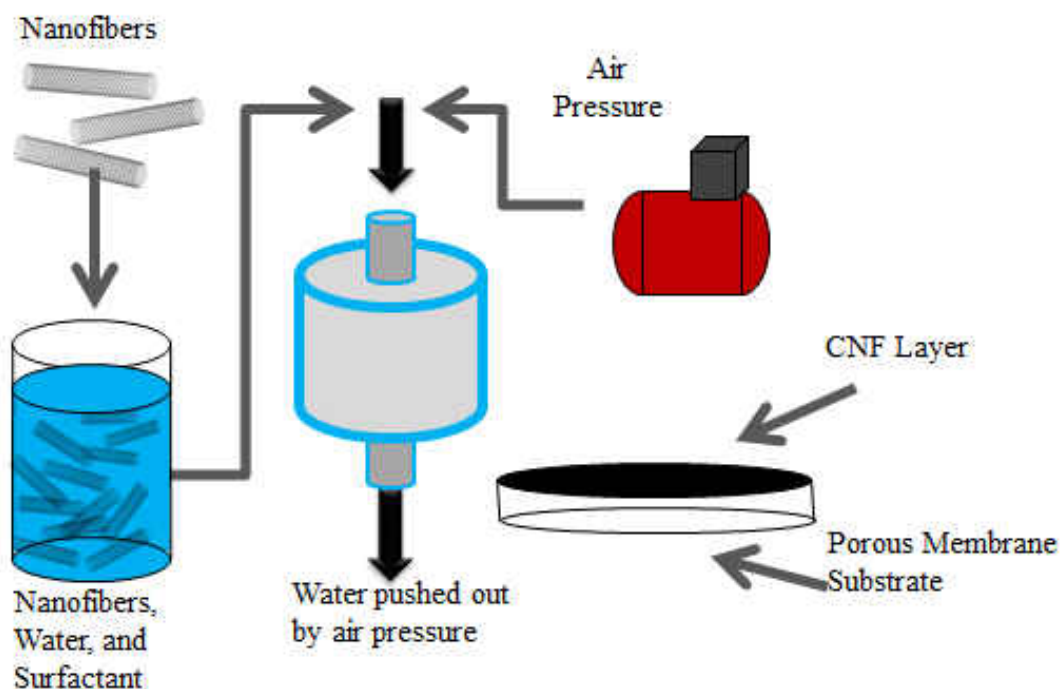


Figure 2 Schematic of Pressure Filtration Method

The two process above both use solutions that use surfactants with ultrasonic mixing. The porous filter paper can be changed to allow uniform distribution of the carbon nanotube network. One alternative to using a solution based method is the frit compression method shown on Figure 3 [19]. Using this method has its advantages such as not having the use surfactants which

affect some of the properties of the nanotubes, and provides larger thickness. These thicknesses are able to range from 120 – 650 μm .

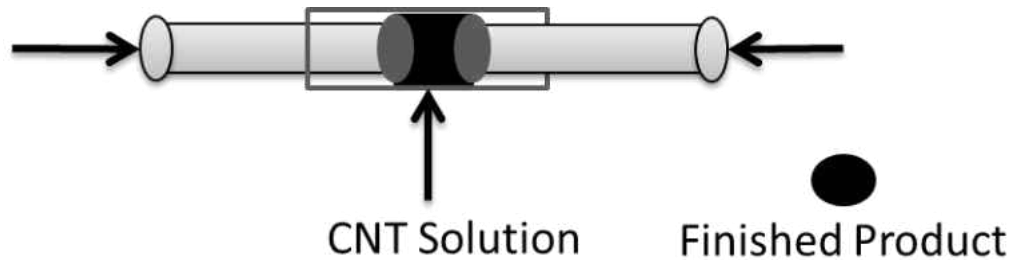


Figure 3 Schematic of Frit Compression Method

The Second alternative is the domino pushing method which works as described. It is an effective macroscopic manipulation of aligned CNT array, which is able to produce CNP [20]. This method is shown in Figure 4 below [20]. This is the only method that is able to ensure that the CNTs are aligned; which provides a lower electrical resistivity compared to other methods.

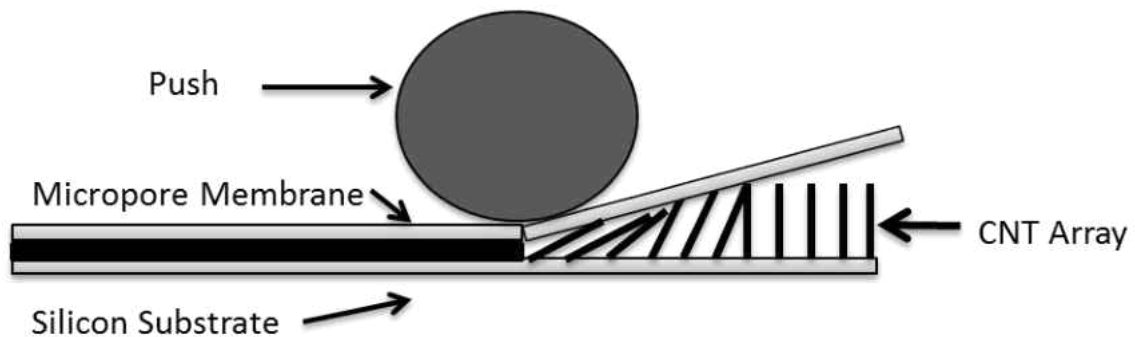


Figure 4 Schematic of Domino Pushing Method

In order to have good electrical conductivity from CNP the nanomaterials have to be tightly packed or aligned. Since it is difficult to align the CNTs is most of the process described above dense packing is needed. Some methods are not able to pack the CNTs densely, but there

is secondary process in which this is able to be accomplished. One example is pressing the CNP after it has been made to improve surface finish, densely compact the CNTs, and giving a uniform thickness. This not only helps with electrical conductivity and thermal stability it also increases the mechanical properties. Pressing with distributed loads shows a sustainable increase in the tensile strength and elastic modulus of the CNP and their composites [21].

2.3 Digital Fabrication Techniques of CNT-Inks

Digital fabrication is a common work used to describe CNC machine that is based off of MIT's 1952 numerically controlled mill [22]. These machines usages range from large to small and cover many different areas. As of right now the latest digital fabrication process is 3D printing and Bio-printing. These two processes do not differ that much from each other. They both are additive manufacturing techniques that combine materials together by stacking layer upon layer until there is a finished product. One method of digital fabrication of CNTs is shown below in Figure 5 which is used in ink jet printers. Figure 5 a shows the thermal technique that is used to produce the CNT ink droplets while b shows the piezo technique. Both are very similar but the piezo is less likely to burn out over time.

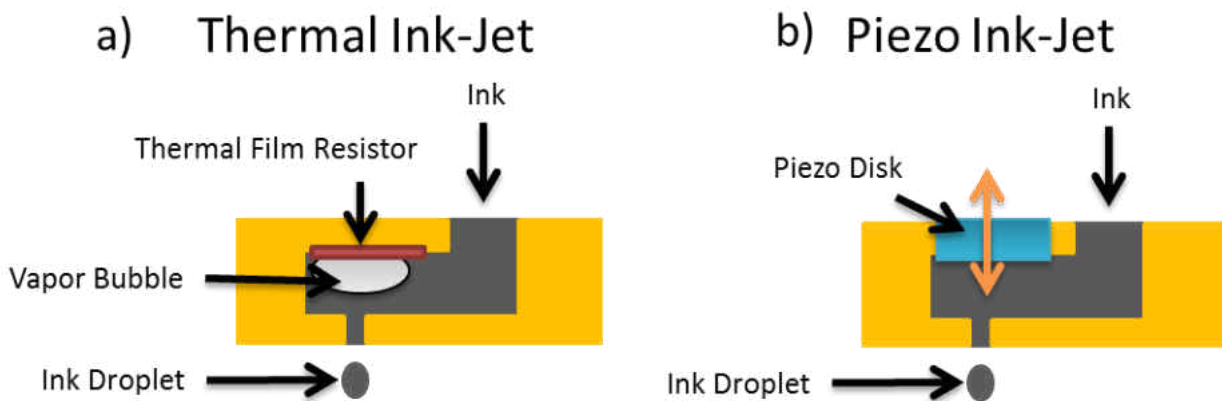


Figure 5 Ink-Jet Processes a) Thermal Jet b) Piezo Jet

Current research is looking into using printers to create flexible electronics with CNT inks. All of these methods use surfactant for the deagglomeration process of the CNTs. The reason for using CNTs is for their incredible electrical and thermal conductivity. For the printing process with an ink jet printer room temperature was used for all of the researchers which was 300 K. Lim et al. [23] found current emission of 536 μA per cm^2 with a bias of 4 V per μm . They also discovered that certain dispersants do not evaporate which lowered the conductivity of the samples. Zhou et al. [24] also discovered that the resistivity changed when different dispersants were used; their values of resistance are $1 \times 10^6 \Omega$ per Square and $3.5 \times 10^3 \Omega$ per square. To increase the conductivity of the samples Tortorich et al. [25] discovered using longer fibers to lower resistance. The chart below shows the increase in electrical conductivity of their work compared to other researchers Song et al. [26] and Fan et al. [27]. This chart shows with the increase in layers the resistance of the sheet will decrease.

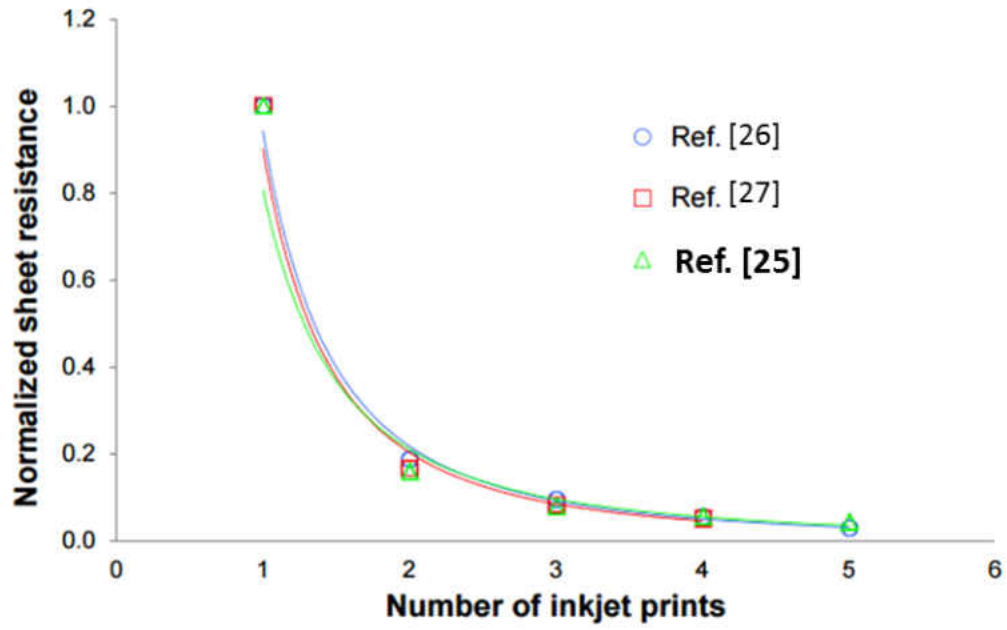


Figure 6 Sheet Resistance Versus Number of Prints [25]

CHAPTER THREE: METHODOLOGY

3.1 Introduction

Carbon nanopaper (CNP) is able to be produced in a variety of ways. Most of the methods used to make CNP is a type of batch method. A batch is a broken operation in which the production has a stop procedure during the operation. Another form of operation that has been looked at in research is to develop a continuous form of CNP. A continuous process is a process that is without interruption during production.

Currently there is only one method that is used for the continuous production of CNP. This is any type of spraying method. Most spraying methods are able to produce a continuous stream of material. They are also easy to use and require low maintenance while in use. Some spraying methods include air blast types (pneumatic and aerosol) or pressure types (piezo, hydraulic, thermal jet, and solenoid). All of these types of sprayers are able to produce an atomized mist, but each of the sprayers has different particle sizes in relation to them. An air blast pneumatic sprayer is able to produce a particle as small as 10 μm , while a solenoid piston can produce particles in the nano size.

Other than the particle size, each type of sprayer also has the ability to produce a type of spray pattern. The types of patterns that can be produced are solid stream, flat spray, hollow cone, and full cone. These types of patterns are shown below in Figure 7 Types of Spray Patterns.

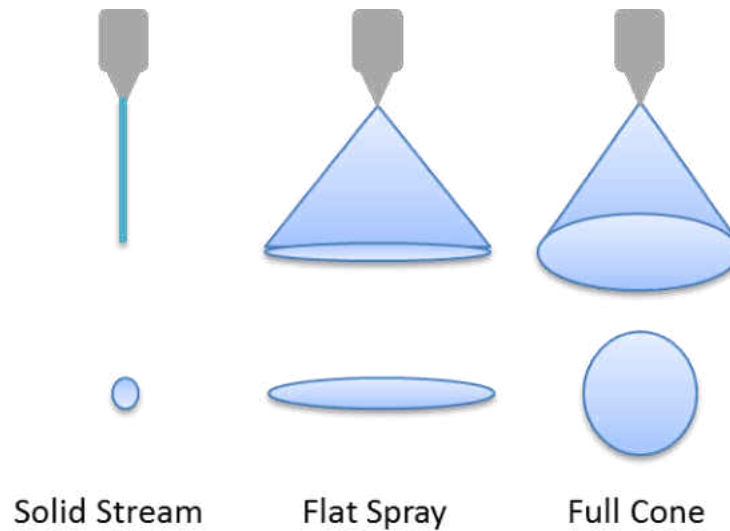


Figure 7 Types of Spray Patterns

In this research only two types of spray patterns are used flat spray and solid stream. The flat spray is used with a pneumatic sprayer on both the continuous spray infiltration method and the resin deposition method. As for SDM a solid stream of particles was used for digital control purposes. This digital control of the stream helps to create digital composites that are able to have more functionality and enhance material properties. The figure below shows how digital composites are able to be created using the SDM process.

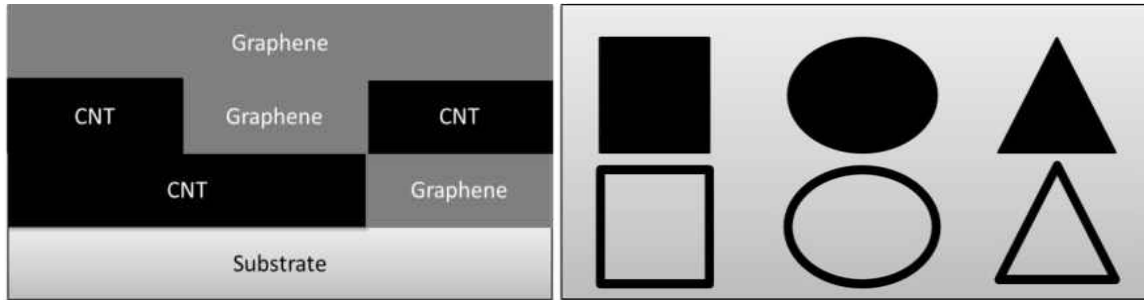


Figure 8 Digital Composite Manufacturing

This digital processing ensures the created composite is geometrically accurate. This process is also additive, which enables the composite to be built layer by layer and has minimum loss of the supplied material.

3.2 Preparation of the CNT-Inks and SMP Resin

Carbon nanotubes are used in many aspects of research and industry for their enhanced material properties. In this research the CNTs are used for their electrical properties. CNTs have a high electrical and thermal conductivity which is used for resistive heating of Shape Memory Polymers (SMP) to encourage actuation. The process in which the CNTs are placed onto the SMP first starts with the creation of the CNT Ink and the SMP resin solution.

Due to the large Vander Waals force holding the CNTs together it is necessary to use a method to deagglomerate them. One method that is used is sonication with dispersant, which uses high frequency and amplitude to force the CNTs apart and the dispersant acts to help to keep the nanotubes from re-agglomerating. Sonication can be used with many types of solvents; the most common is ethanol and water. The water solvent used in the CNT ink has a stability for half an hour; where the CNT ink with the ethanol solvent has a stability for 1-2 weeks.

Preparation of the CNT inks for the spray infiltration method starts with a 1 to 1 solution (1 gram of CNTs to 1 Liter of water). Then 10 drops of triton X-100 surfactant is deposited into the solution and sonicated for 35 minutes. There are two types of CNT inks for the SDM process one has an ethanol solvent and the other has water as a solvent. The water base SDM CNT ink is closely related to the spray infiltration methods CNT ink, but the formulation is slightly different. Instead of using a 1 to 1 solution a 1 to 0.15 solution is made (1 gram of CNT to 150 mL of water). The same amount of surfactant drops are used for this ink with the same sonication time. The ethanol solvent based ink uses a ratio of 1 gram of CNTs to 150 mL of ethanol with 2 mL of Disperbyk, which is a type of dispersant. This solution is sonicated for ten minutes then replenished with ethanol to refill the 150 mL solution. This loss is due to the heat that is generated during the sonication process. After the material has been replenished sonication is done one more time for ten minutes. Then the solution is placed into 450 mL of ethanol to lower the viscosity.

SMP resin is produced by dissolving SMP pellets with a Tg of 55°C into N,N – dimethylformamide (DMF) at a temperature of 50°C. The temperature is generated by a hot plate and when the material is fully dissolved it is stirred for 3 hours. The solution produced is 10 wt% SMP.

3.3 Spray Infiltration Method

Spray infiltration process for the fabrication of CNP involves atomizing the inks into fine droplets, which is directly sprayed onto the cellulose filter paper. This cellulose filter paper is on a continuous moving belt that has an adjustable speed value. The speed ranges from one inch per minute to nine inches per minute. A heater is also on the machine to dry the paper after it has been infiltrated with the water based CNT ink.

3.3.1 Spraying Method

The spray pattern that is used for this process is a flat spray pattern. This pattern is reliable for creating continuous samples with uniform thickness and distribution. The figure below shows the distribution for a pneumatic air blast pattern. The pattern is evenly distributed over the center area, but decreases at the ends. To compensate for this decrease the pattern is over sprayed an inch on each side of the paper to provide an even distribution for the entire CNP.

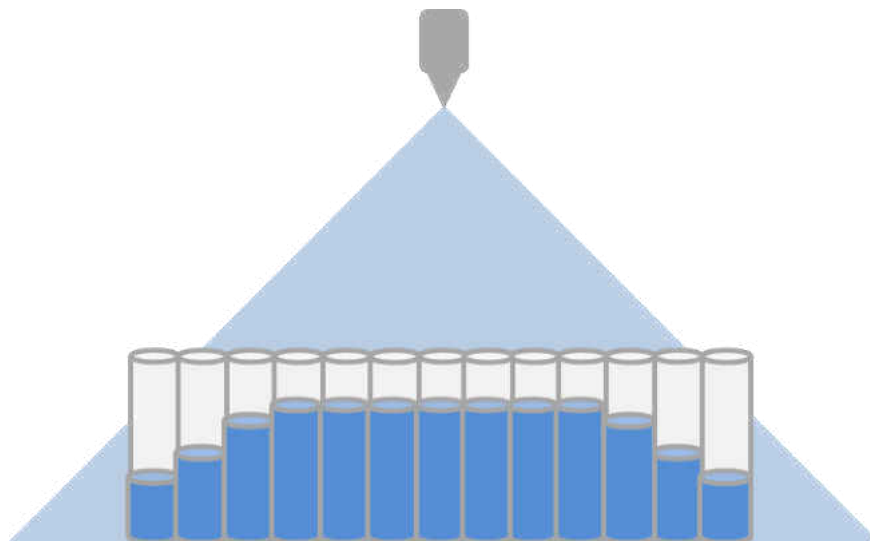


Figure 9 Pneumatic Spray Distribution Schematic

The distribution of the material also has to do with the flow rate of the ink. The flow rate for this method is 0.14 liters per second. The flow rate is directly dependent on gravity which feeds the material into the air blast zone. The particles that are generated by this air blast are as small as 10 μm . The size really depends on the air pressure released and the viscosity of the CNT ink.

3.3.2 Fabrication Process

Due to the ease of production for the spray infiltration method the scalability of this process is very simple and easy. The rate of production is able to be increased by adding more pneumatic sprayers. With the addition of one extra sprayer the production rate should increase by two times the current amount. But there are some issues that have to be addressed when doing this. The amount of air given to each nozzle has to be the same, so an increase in air pressure has to be supplied. Another issue is the vacuum rate has to be increased as well, or the chamber has to be extended with more vacuum chambers to allow for the increased flow rate that is generated by the addition of more nozzles. Current fabrication process of the CNP is shown below in Figure 10. This figure shows the entire process from the creation of the CNT ink to the end product.

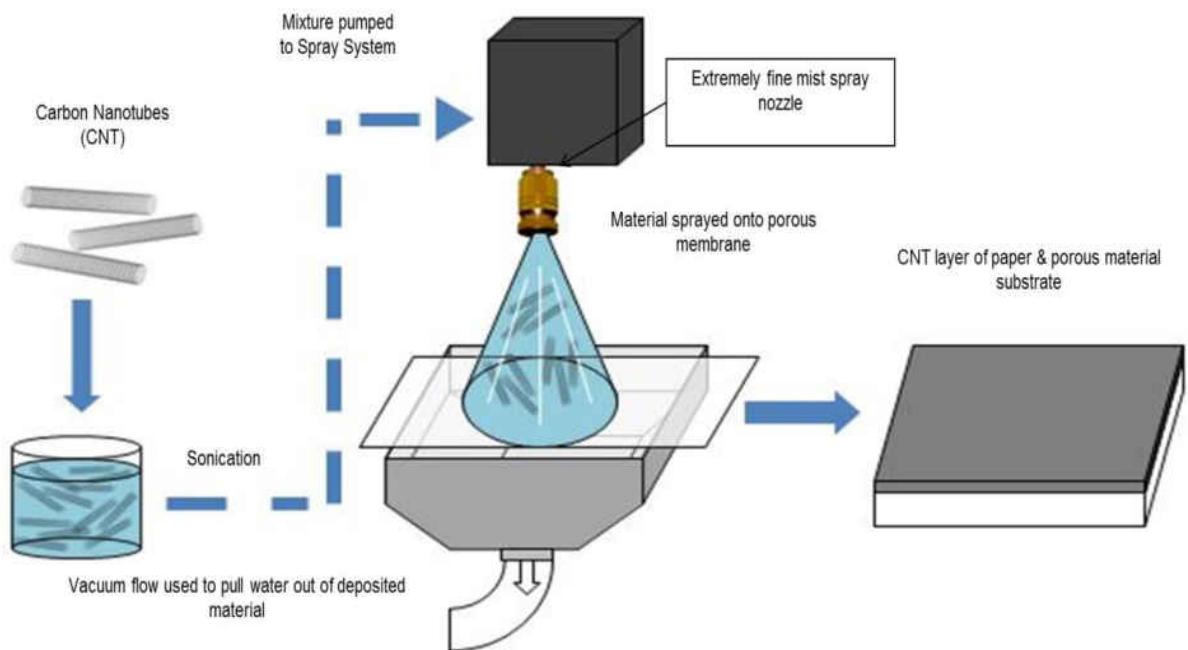


Figure 10 Spray Infiltration Fabrication Process

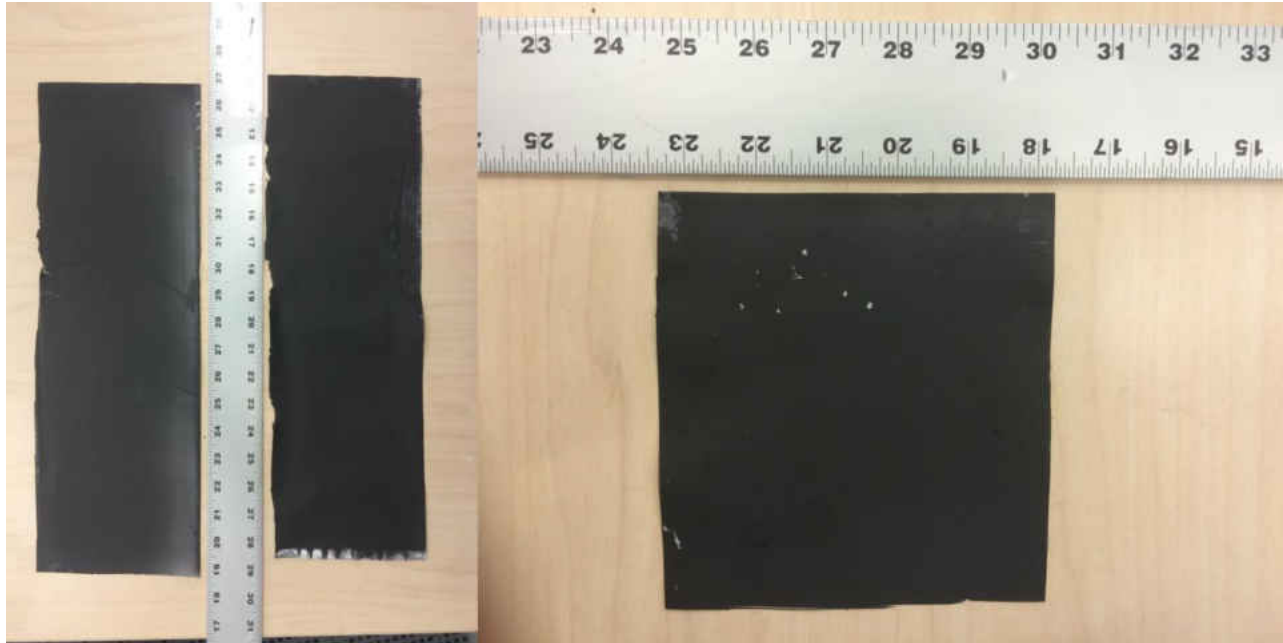


Figure 11 Samples Produced by Spray Infiltration Method

Products produced by spray infiltration method are shown above in Figure 11. This figure has three samples two are 6 x 18 inches and the other one is a 6 x 6 inch sample. The 18 inch sample shows the continuous production ability of the machine; while the smaller sample shows the quality that can be obtained. These samples were done at separate production rates to maximize the amount of material that was used. The larger samples were produced at a rate of six inches per minute while the smaller sample was produced at a rate of two inches per minute.

3.3.3 Processing Effects



Figure 12 Processing Effects of Spray Infiltration using Cellulose Filter Paper

Figure 12 shows one of effects during the processing of the CNP. This tearing of the CNP is caused by overlapping on the sides of the cellulose paper and the vacuum chamber. This tearing also causes leakage of the vacuum which has its own effects. Some other effects during processing are complete vacuum and incomplete vacuum. Complete vacuum is where there is no leakage for the air to penetrate through and clogs the vacuum chamber. This clogging keeps the belt form moving. The last processing effect is incomplete vacuum which can occur when the cellulose paper tears as shown above or when the vacuum chamber is receiving too much air. These two effects mentioned causes the CNP to be non-uniform which lowers the quality of the paper and the material properties of the CNT. Incomplete vacuum also causes the material to pool in areas which also creates non-uniform CNP.

3.4 Spray Deposition Modeling

Spray deposition modeling is a digital fabrication process in which the CNT ink droplets are supplied in the form of a stream to any desired location because the nozzle is connected to a computer controlled x and y axis. SDM is similar to an ink jet printer, but SDM has the ability to model over the same area with precision accuracy. Since the substrate does not move the supplied inks always goes in the desired location. This particular method also allows for a variety of substrates to be used. Another advantage is environmental control. The system has a built in vacuum system and heater for enhanced evaporation and processing of the inks.

3.4.1 Spraying Method

Thermal jet also known as “bubble jet” is a common form of ink jet printing and has been used to deposit CNT inks onto PTE substrates. This type of digital fabrication process is desirable because the nozzles are controllable by a frequency and are mass manufactured with multiple nozzle outlets. A bubble jet nozzle with a 12 nozzle array and 235 μm pore size is used in SDM. This allows for a large enough pore size to keep the nozzles from clogging while creating particles that are small enough to dispense the CNT inks properly. The highest frequency for this nozzle is 1250 Hz. This is largest frequency value before the resistors inside the nozzles burn out.

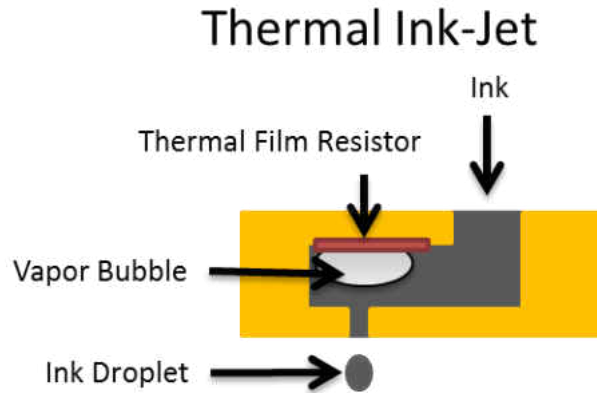


Figure 13 Spray Deposition Modeling's Spraying Method

The figure above shows the thermal jet nozzle and how it works. Inside all of the nozzles are small resistors that are able to be heated due to resistive heating when voltage is applied to them. When the resistor heats up it causes the liquid inside the chamber to heat and become vapor. This vapor then forces the material closest to the exit to escape.

3.4.2 Fabrication Process

Digital Processing of CNP with nano-inks is accomplished by the process shown on Figure 14. This figure shows the entire process from the sonication of the CNTs to the final product. After the sonication of the CNTs in either water or ethanol the material is then placed into the thermal jet nozzle to be sprayed on to the substrate. The substrates that are able to be used are copper, aluminum, steel, SPM, cellulose paper, and others. The substrate is then heated with a heat plate that is located below. While the substrate is heated the nozzle sprays the material in the order given by the G-code. Vacuum is able to be applied if the flow rate is too high or if the speed is too slow. The speed is able to be changed in the G-code, to speed up or slow down the printing process. If the speed is slower a more material is placed in the same area which will give a thicker more conductive sample.

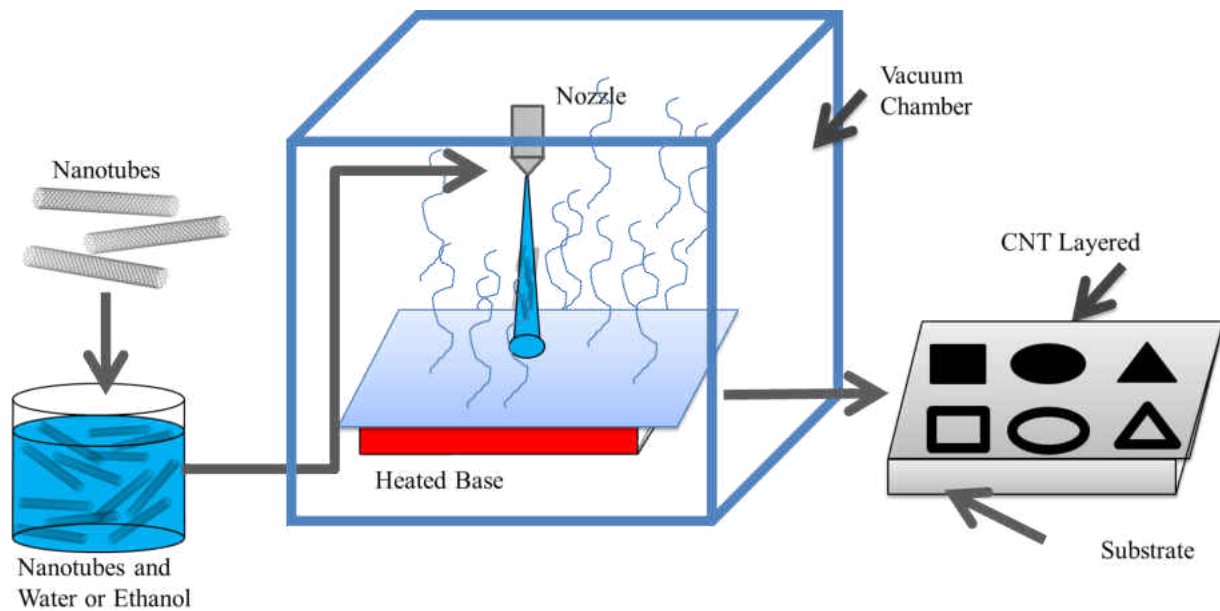


Figure 14 SDM Fabrication Process



Figure 15 Samples Produced by SDM Process

Products produced by spray deposition modeling are shown above in Figure 15. This figure has three samples each on different substrates, which shows one of the capabilities of the printing process. The first image in the figure above was done using the water based CNT ink while the other two were done using the ethanol based ink. Two of the images above show the geometric control of SDM.

3.4.3 Controls

Spray deposition modeling uses computer numeric controls (CNC) to move the nozzles into position and allows the thermal jet nozzle to lay down the material properly. The machine runs on G-code, which is a type of code that can be translated into machine code easily. A MATLAB code was made to bring in 2D images and generate G-code interoperation of the image.

G-code is used in many machines to move up to six axes and control the tools that are provided for those machines. In SDM G-code is used to move the two axes and control all 12 nozzles individually. Another type of code was made to process the nozzle control called “A-code”, which is used to fire the nozzles. How to write the codes and what they mean is located in Appendix A.

MATLAB was used to write the G-code for the SDM by taking 2D images and making them into binary, which gives the exact locations of where the CNT ink needs to go. To simplify the process only black and white images were used. Figure 16 shows some plots generated by the MATLAB code. Figure 16 a shows how the thermal jet nozzle moves during the printing process and b shows each location that the droplets will be released. For this figure only 3 nozzles were used. Appendix B shows the MATLAB code that was used to create the images below and the G-code that was generated for this image.

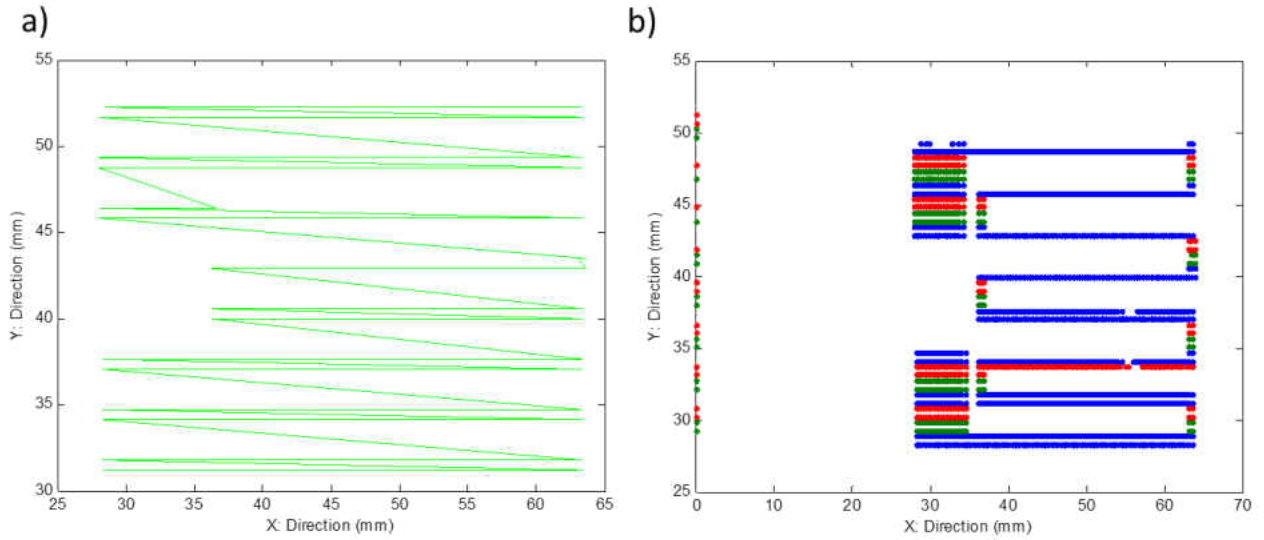


Figure 16 G-Code Processing in Matlab a) Nozzle Travel b) Droplet Pattern for 3 Nozzles

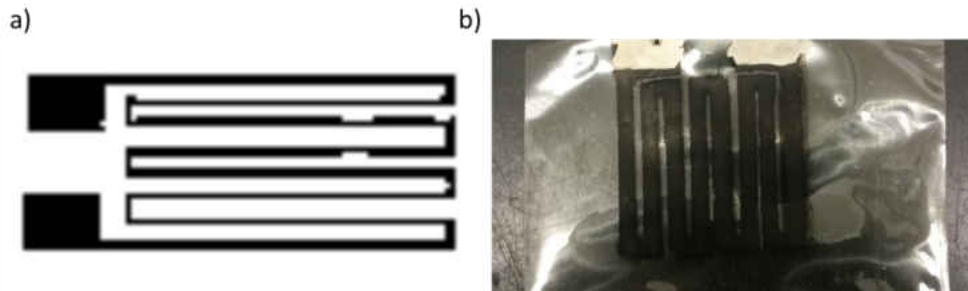


Figure 17 a) Black and White image of the Model b) the printed model

The black and white image shown in Figure 17 is the image used to generate the plots shown in Figure 16. The image correlates closely to the plots generated. Figure 17 b is a sample of the model after it has been printed.

3.4.4 Processing Effects

In every process there are effects that occur, for SDM a major effect is clogging of the nozzles. This is due the agglomeration of the material over time. Other causes for clogging are incorrect placement of the nozzle, if ink is too thick, and if the nozzles are not purged over a

period of time. Incorrectly placing the nozzle causes the material to exit the nozzle incorrectly, which causes pooling of the material which blocks the exit. If the ink is too thick the material simply is not able to exit the nozzle. This also causes clogging in the chamber and can cause the nozzle to burn out. Due to heating the chamber purging is needed to keep the material from sitting inside the nozzle for too long and causing the solvent to evaporate, which causes the nozzles to burn out.

Another problem for this nozzle type is leakage. This effect happens when the materials viscosity is too low. The major effect from this is that the nozzles are not able to create particles because the surface tension at the exit is not high enough to allow for the material to be forced from the exit.

3.5 Resin Deposition Method

3.5.1 Film Fabrication

Film fabrication is done by taking the CNP that is made by either spray infiltration process or the SDM process and applying a coating of SMP resin on it. There are several parameters that are controlled during the processing of the films. The first is the flow rate of the SMP resin that is air blasted onto the substrate below and the other is the speed at which the belt is moved to allow for buildup of the resin. By moving the belt faster or slower the thickness can be controlled. The faster the substrate moves the thinner the product.

The process of film fabrication is done slightly different for either spray infiltration or SDM processes. For SDM an aluminum plate is coated with thick layer of SMP resin first before it goes through the SDM process. After the SDM process is completed another coating of resin is applied to the top.

Below Figure 18 shows the process for the film fabrication of spray infiltration creation of CNP. For this process the CNP is sprayed on the cellulose side. The DMF in the resin dissolves the cellulose and only SMP and CNT are left behind. Another coating can be placed on the CNT side as well to give a self-standing CNT SMP film that can be used for resistive heating of the SMP for actuation purposes.

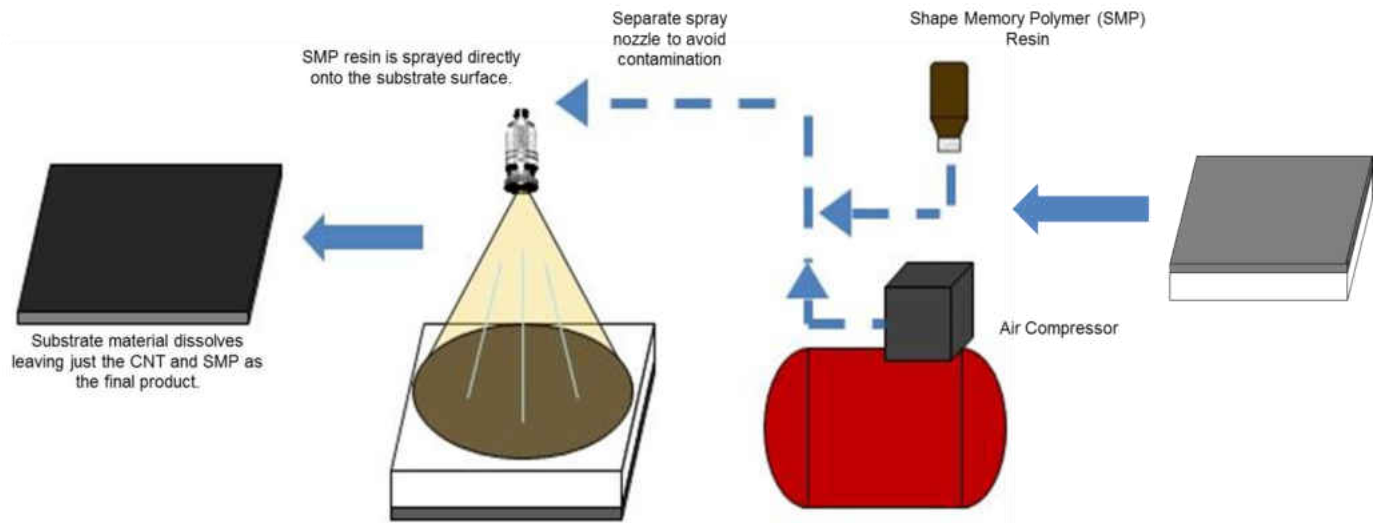


Figure 18 Film Fabrication of Spray Infiltrated CNP

Below are some samples that were obtained by the process that is shown in Figure 18. There is uniformity throughout the film and after it is released from the substrate it is self-standing with no wrinkles in the last two samples. The first sample was not placed in the oven fast enough and wrinkles occurred during the dissolving of the cellulose paper.



Figure 19 Film Fabrication of Spray Infiltration CNP



Figure 20 Film Fabrication of SDM

Figure 20 shows the final product of the SDM film processing. The film in the center only has one side sprayed to keep the electrical conductivity high and to prevent the resin from infiltrating the CNTs. All the films produced were uniform in thickness and in area coverage.

3.5.2 Processing Effects



Figure 21 Processing Effects of Depositing Resin

Figure 21 shows the processing effects that occur during the film making process. The only major issue during the processing of CNP was over coating. The first image in the figure above shows that when only one coating is done there is still cellulose paper that has not dissolved by the DMF. After another coat has been placed a finished product is given. The final image shows what happens if more than two coats of resin is applied. This is due to the shrinkage of the material during the heating process. If there is no more cellulose for the material to penetrate into it coats the top and begins to shrink.

CHAPTER FOUR: TESTING AND EVALUATION

4.1 Introduction

Characterization of machines and components are required to know what it is capable of and how it is able to be used properly. In this study the cauterization of spray infiltration method with and without film fabrication, and SDM with and without film fabrication was done to find the parameters that are needed to be set for everyday use. For both processes several techniques were used to find the parameters that are able to be set. The major parameters for both of the processes are electrical conductivity, weight of the ink distributed to the sample after processing, and heating due to electrical resistivity. Other parameters that were found include total loss due to spraying and thickness of the produced CNP.

One of the major parameters found for both processes is electrical resistivity of the fabricated films. This resistivity is a necessary value to correlate the speed at which the material is deposited and the resistivity of the product. This value is also needed for the resistive heating of the film for use with electronics or SMP shape actuation. The figure below shows the test that was administered to find the resistivity values. This method is known as the four point probe resistivity test. This test uses voltage and current to calculate the resistance of the sample. To find the resistivity of the film in terms of $\Omega \cdot \text{cm}$ the thickness is required. The equation for that is $\rho = 4.53 * \frac{V}{I} * t$, where ρ is the resistivity in $\Omega \cdot \text{cm}$, t is the thickness of the sample, V is the voltage, and I is the current.

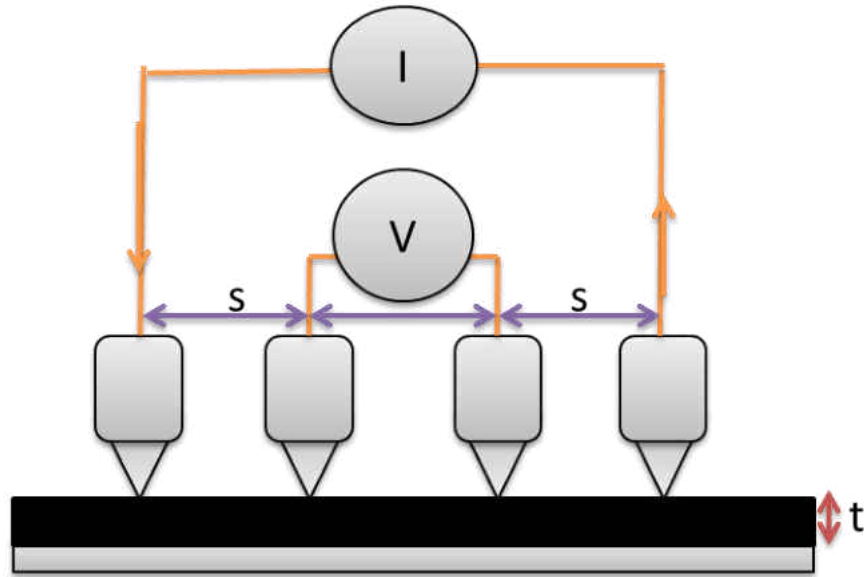


Figure 22 Schematic of the Four Point Probe test for Resistivity Measurements

A scanning electron microscope (SEM) was used to find the thickness of the material deposited and to see how compact the CNTs were. Using the SEM allowed the thickness to be found, which could then be used to correlate the speed at which the material was deposited to the thickness generated. This characterization of the spraying process allows for complete control of the thickness and the resistivity that is desired from the manufactured CNP.

During the processing of the CNPs weights were taken to find a correlation of the weight distributed and the speed at which the material was dispersed. For the spray infiltration process the weight of the cellulose paper was taken before it was sprayed and then the weight was taken after to find the exact weight of the CNTs distributed onto the cellulose filter paper. To find the weight of the material that was distributed from the SDM, aluminum foil was used and it was weighed before and after as well. These weight values help to correlate the speed of the machine to the weight.

4.2 Spray Infiltration Method

4.2.1 Electrical Resistivity

To find the electrical resistivity of the spraying infiltration method the film fabrication process was done first and then the four probe resistivity measurements were taken. Five measurements were taken from each sample and averaged to give the results in the chart shown below. This chart shows a linear trend for the thickness to resistance measurements.

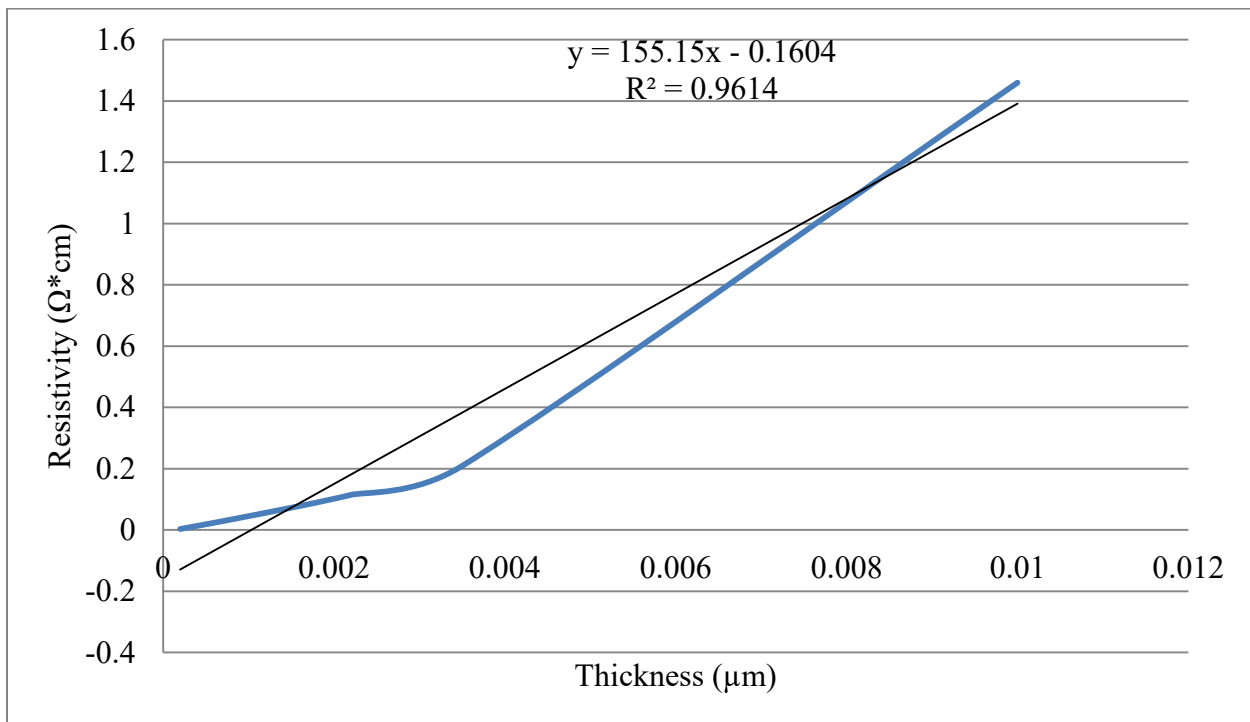


Figure 23 Electrical Resistivity Measurements for Spray Infiltration Method

The five values taken from each sample were plotted and shown on Figure 24. All of these values taken were closely related suggesting that the entire paper was uniform in thickness. The only exception was the sample that was produced at nine inches per minute. This sample had huge variations showing at higher speeds inconsistency in the thickness and distribution of the material were seen.

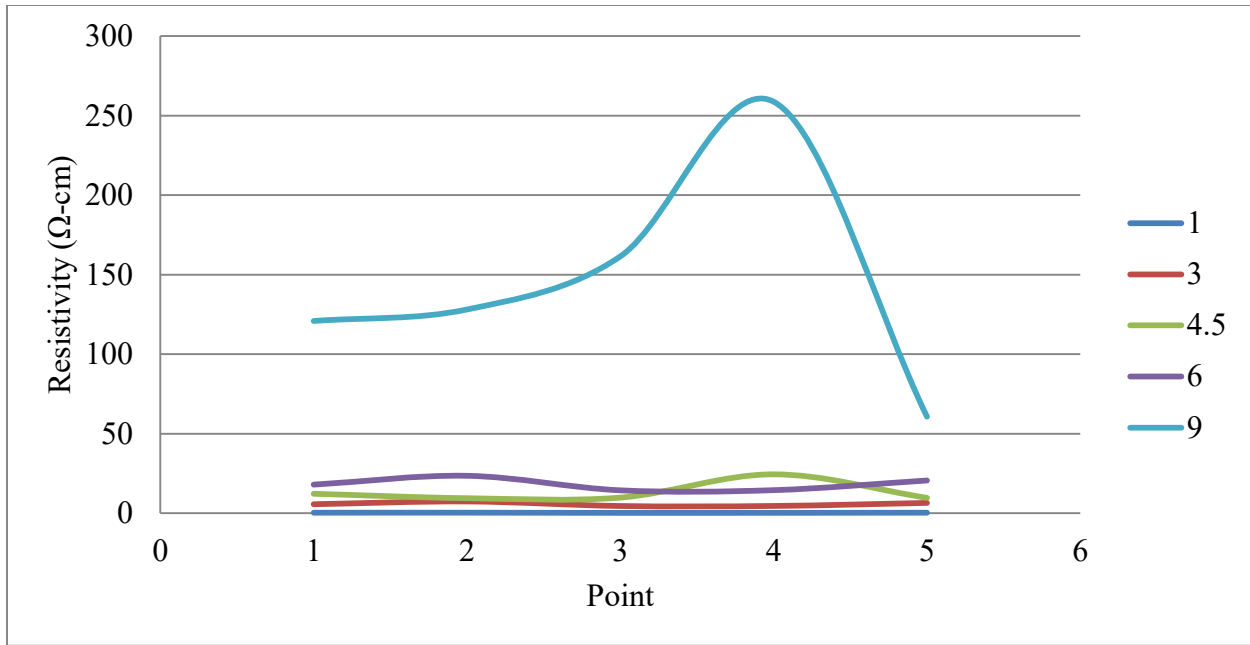


Figure 24 Resistivity Measurements over the Area

Table 1 shows the values that were measured and calculated for the resistivity of the film produced. These values are used in the charts above, which show the linear relationship of speed to resistivity and thickness to resistivity. Some values that were not shown on the chart are also listed below. These values are the resistivity in Ω per square which is the given values from the four probe resistivity test with an uncertainty of $\pm 0.005 \Omega$ per square. The thickness was used to calculate the resistivity in $\Omega \cdot \text{cm}$ from the equation shown in section 4.1.

Table 1 Resistivity Measurements for Spray Infiltration Method

Speed (inch per minute)	Thickness (μm)	Resistivity ($\Omega*\text{cm}$)	Resistivity (Ω per square) ± 0.005
1	100	0.002874	14.394
3	35	0.050192	45.712
4.5	22	0.114331	52.066
6	11	0.208687	59.334
9	2	1.459663	146.042

4.2.2 Thermal Testing

Using resistive heating (Joule heating) the maximum temperature for a given sample could be found. For this experiment 25 VDC was used as the starting point to find the heat generated and the current value that was associated with the voltage applied. The reason for using 25 VDC was to use low energy to produce high temperature, due to the fact that most power supplies are 12, 24, or 36 volts DC. The figure below shows the heat distribution and the maximum amount of heat that was generated by the 25 VDC.

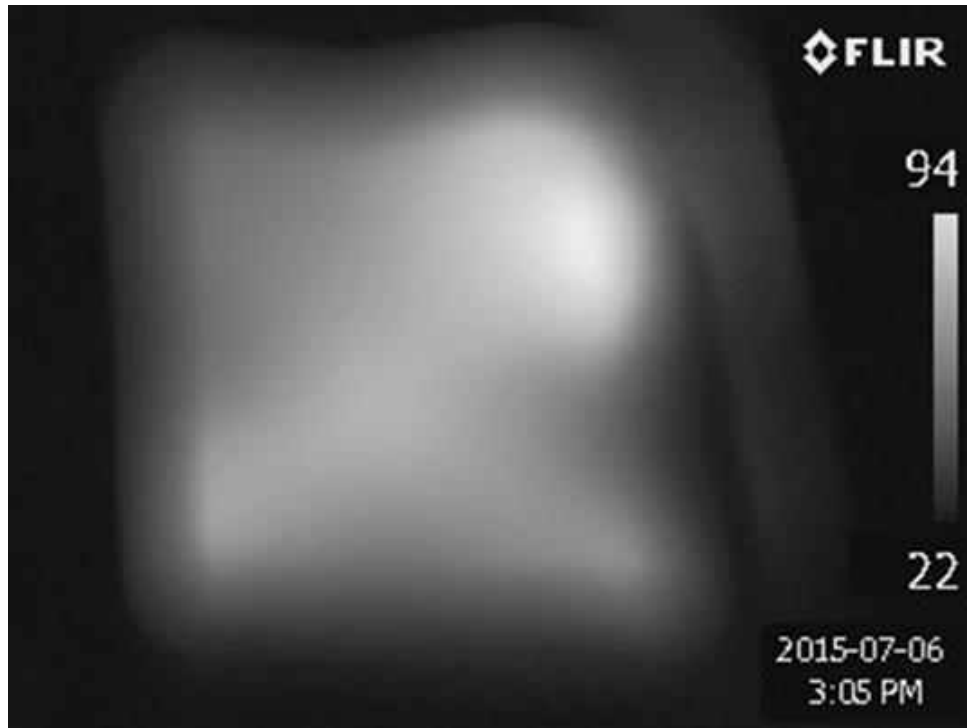


Figure 25 Thermal Image of the Spray Infiltration Sample

The current was plotted against the temperature to find a trend of the heating relationship to resistivity. Figure 26 shows a linear relationship for temperature to current. This also shows that the resistance would be linear as well because $V=IR$, where V is voltage, I is current, and R is resistance. Using this relationship, the maximum temperature the film can produce at any voltage is able to be found.

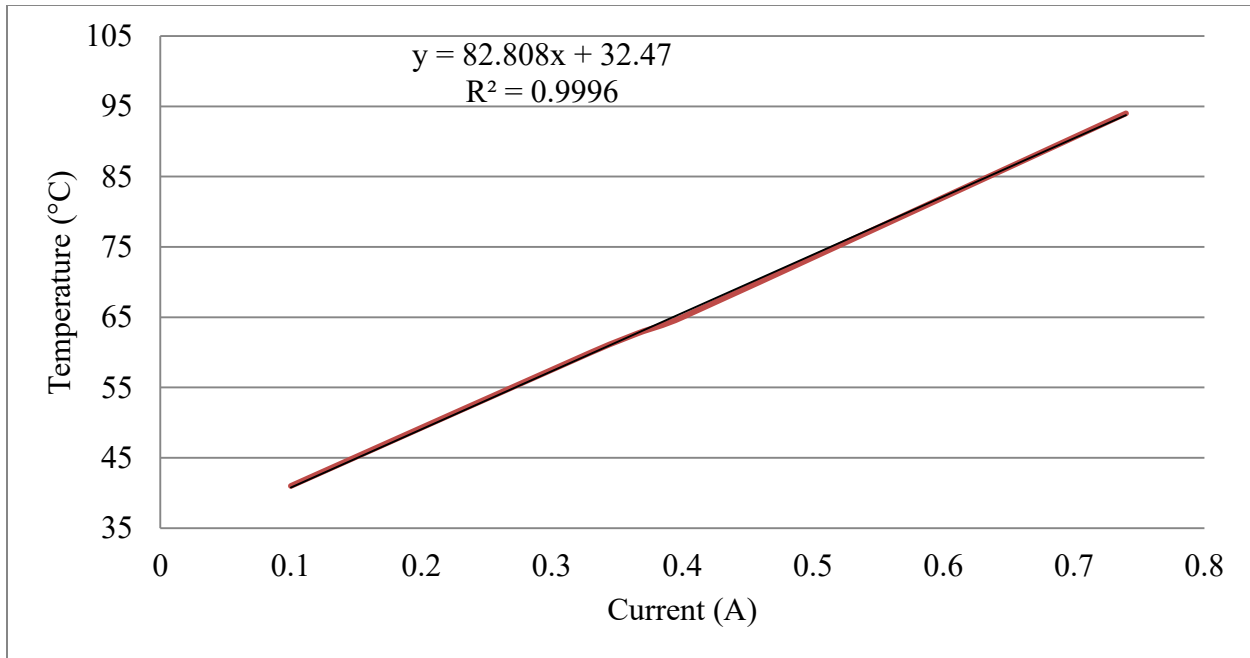


Figure 26 Temperature vs. Current Measurements for Spray Infiltration Method

Using Ohm's law the resistance of the sheet was able to be calculated. Some of the values used had some uncertainties these uncertainties are due to the values given by the equipment used. Using a power supply that was able to show the current had an uncertainty of ± 0.005 A, with a voltage unknown of 0.05 VDC. The thermal camera has an uncertainty of $\pm 0.5^\circ\text{C}$.

Table 2 Thermal Measurements for the Spray Infiltration Method

Speed (inch per minute)	Current (A) ±0.005	Temperature (°C) ±0.5	Resistance Calculated (Ω)
1	0.74	94	33.78
3	0.4	65	62.5
4.5	0.37	63	67.56
6	0.33	60	75.75
9	0.1	41	250

4.2.3 Thickness Measurements

One of the most important characterizations of the spray infiltration process is the thickness. To find the thicknesses, SEMs were done on all of the samples that were made using different velocities. One of the SEMs is shown below as Figure 27. The corresponding velocity for this sample is one inch per minute. This was also the thickest sample that was generated. The total thickness is slightly over 100 μm. The smallest thickness is around 2 μm and its resulting velocity was nine inches per minute.

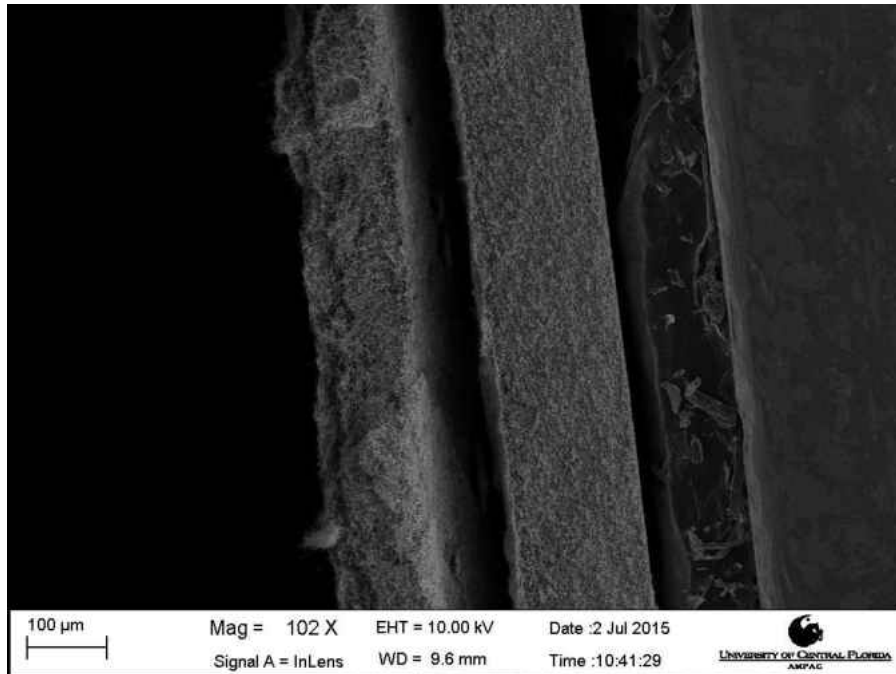


Figure 27 Cross Section SEM Image of the 100 μm CNP

Figure 28 below shows an exponential decrease of the thickness to speed ratio. The reason for this decrease is due to the loss of the material during spraying, but also is able to be contributed to the amount of material that is able to be released during that time. As the speed increases less material is sprayed, so the lower the weight and the lower the thickness. The trend line that is an exponential curve is able to be used to characterize the infiltration process and be used to find the thickness for any speed.

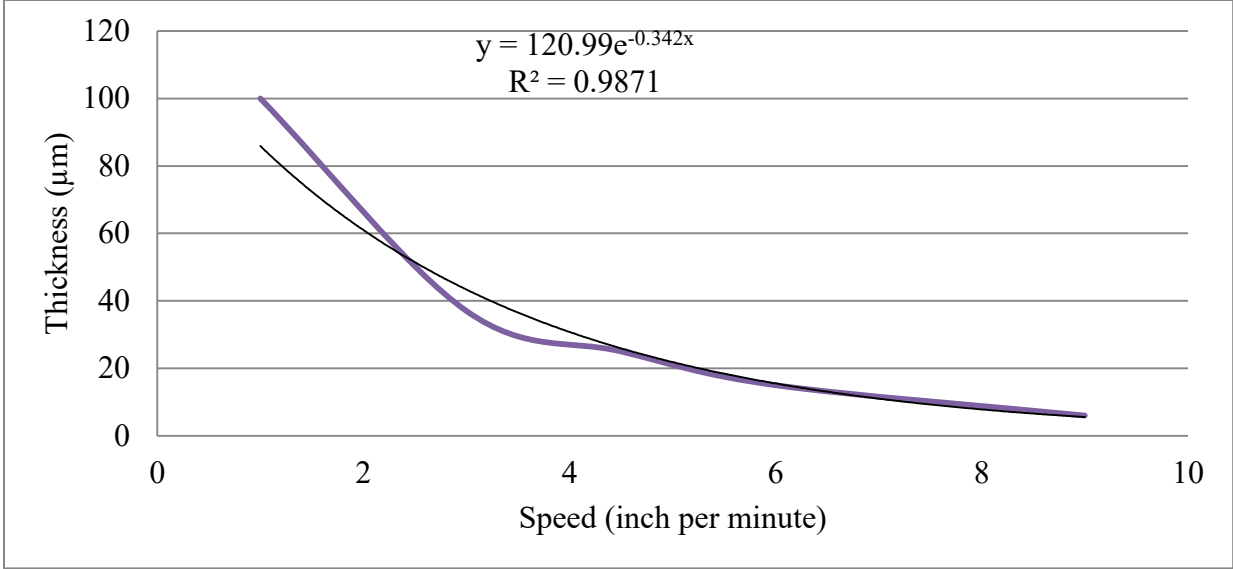


Figure 28 Thickness vs. Speed Chart for the Spray Infiltration Method

The resulting values are shown on Table 3. This table shows the thickness and its corresponding velocity values. There is an uncertainty of $\pm 2 \mu\text{m}$ for the speeds less than six inches per minute. This uncertainty is due to visual accuracy of the SEM image. For the nine inches per minute sample the uncertainty is $\pm 0.5 \mu\text{m}$, this value comes from the zoom of the SEM, which was $2 \mu\text{m}$. A pixel ruler was used to get the values shown below.

Table 3 Thickness Measurements for the Spray Infiltration Method

Speed (inch per minute)	Thickness (μm)
1	100
3	35
4.5	22
6	11
9	2

4.2.4 Weight Measurements

Another major characterization parameter is the weight of the material distributed on to the cellulose filter paper. Using logarithmic equation generated by the trend line the weight is able to be determined by the speed of the machine. The trend line does not follow the curve exactly which is due to the loss generated by over spraying. This also could be contributed to a number of other factors listed in chapter three.

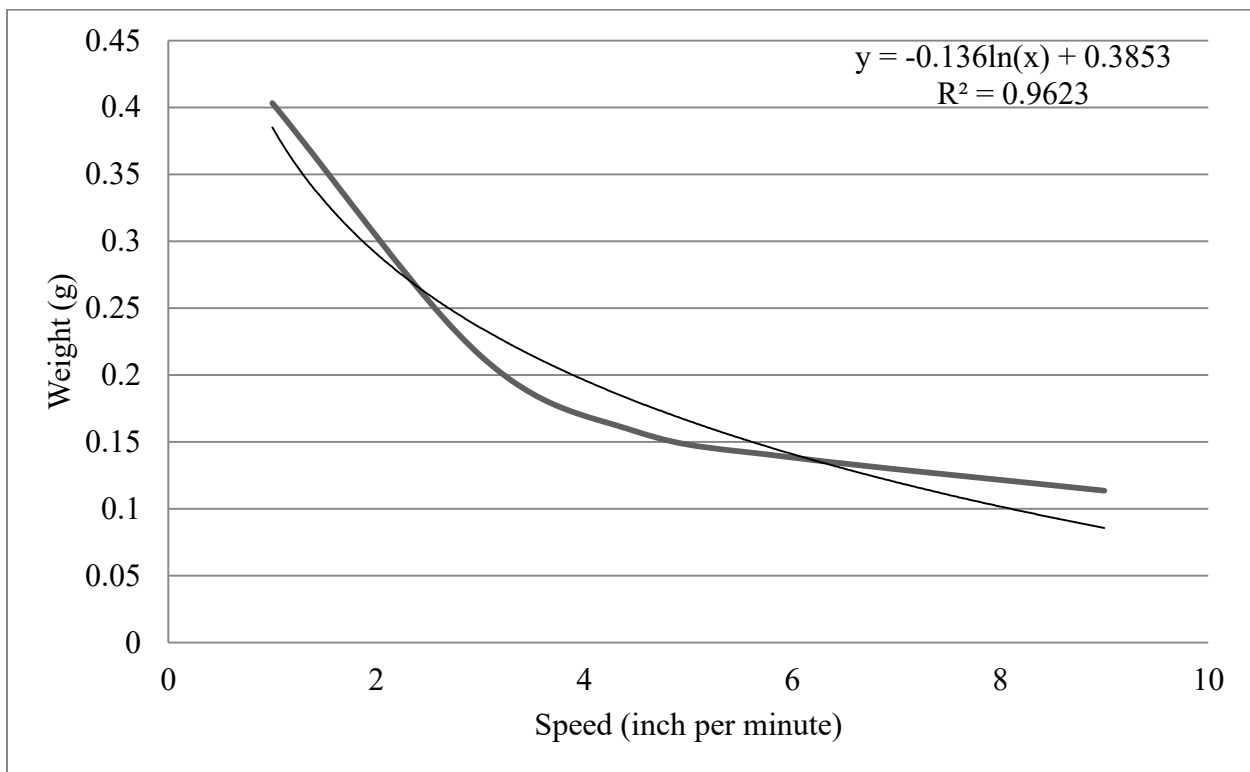


Figure 29 Weight vs. Speed Measurements for the Spray Infiltration Method

To determine exactly how much material is lost due to over spraying and leakage the volume of the deposited material was plotted versus the weight of the CNP which is show on Figure 30. This figure has a completely linear trend with little variation which shows that the losses of the material due to those facts are small.

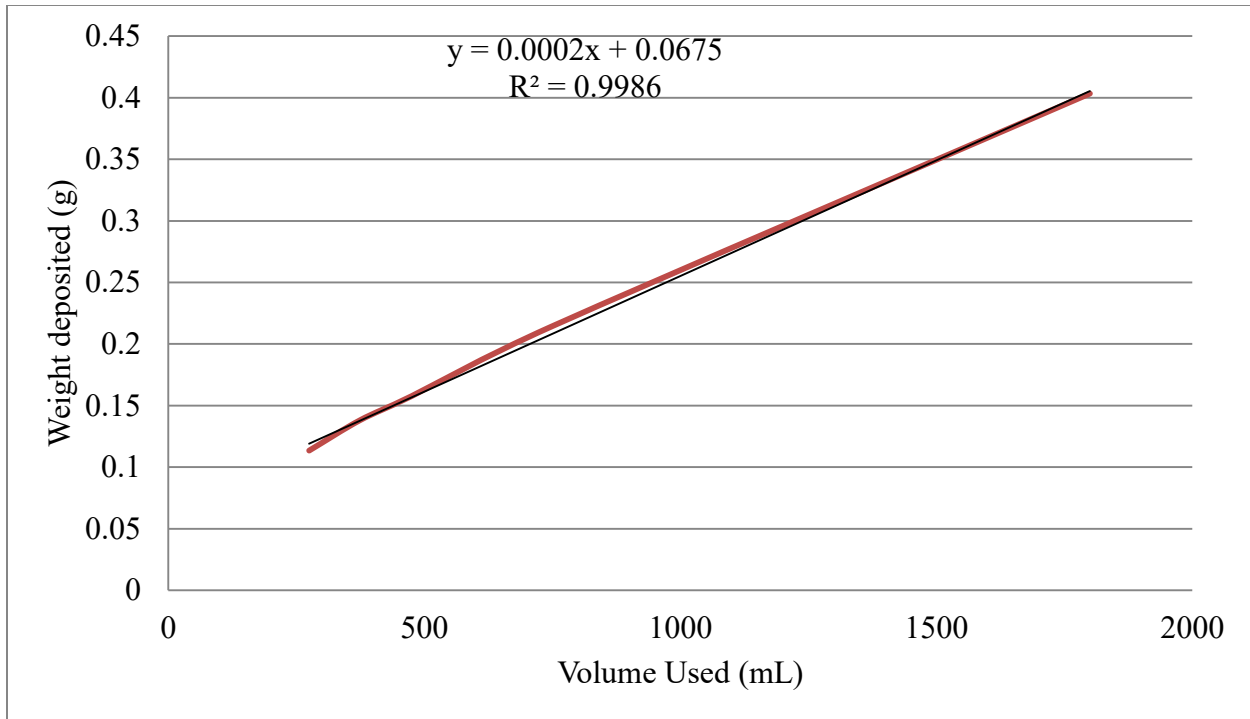


Figure 30 Weight vs. Volume Measurements for the Spray Infiltration Method

The volumetric measurements were taken by measuring the material before and after spraying. By knowing the amount of material going in and the leftover amount after spraying a difference can be taken and that amount is the amount that was deposited. After doing this for every sample a linear trend was found. The uncertainty for this measurement was ± 50 mL.

4.3 Spray Deposition Modeling

4.3.1 Electrical Resistivity

SDM processing has shown some major advantages over other machines like ink jet printers. One major advantage of SDM is the decrease in electrical resistivity which is shown in the figure below. The plot shows an exponential decrease of resistivity as the number of layers is

increased. This is due to the compacting and further distribution of the nanotube network. The trend line has an R^2 value of 0.9764 which confirms the linearity of the resistance.

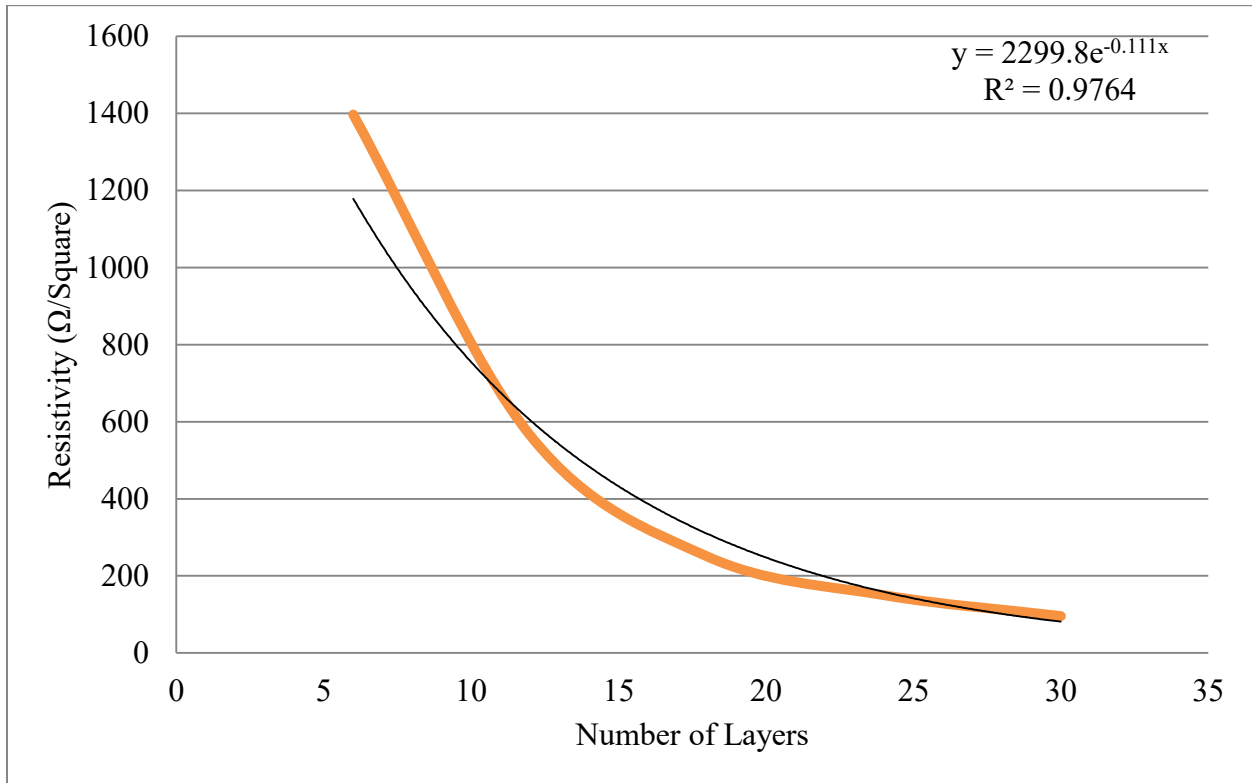


Figure 31 Electrical Resistivity Measurements from Layering

In order to find the resistivity the four point probe test was done on three sections for each of the samples. The trend for each of the samples is shown below. All of the samples except for layer number six are linear with a little variation. The exception had a single value that was larger than the rest. This is due to having a small amount of nanotubes on the substrate.

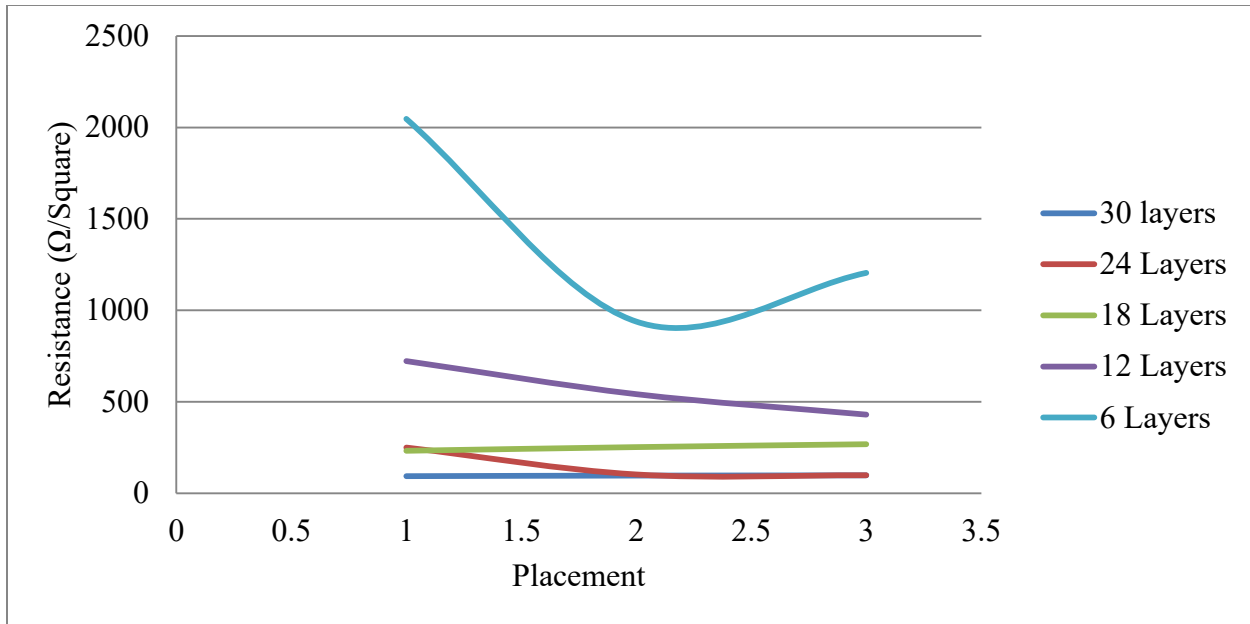


Figure 32 Electrical Resistivity of each Layer over the Distance for SDM

The uncertainty of gathered measurements is $\pm 0.005 \Omega$ per square which is contributed to the lowest value set by the probe. Other uncertainties come from the measurement itself, so more than one measurement was taken and then the average of this was used. Another uncertainty is the actual distribution of the material because of the pauses during printing at the ends of the sample.

4.3.2 Thermal Testing

Joule heating of the material is very important for this process to actuate SMP thin films and provide an even distribution of heating to the sample. The maximum temperature of the sample shown below in Figure 33 is 102°C . In this experiment 237VAC was used as the starting point to find the heat generated and the current value that was associated with the voltage applied. The reason for using 237VAC was due to the high amount of resistance produced by SDM processing. The figure below shows the uniform heat distribution which resembles that of an

oven heater, and the maximum amount of heat that was generated by the 237VAC that was applied to the thin film.

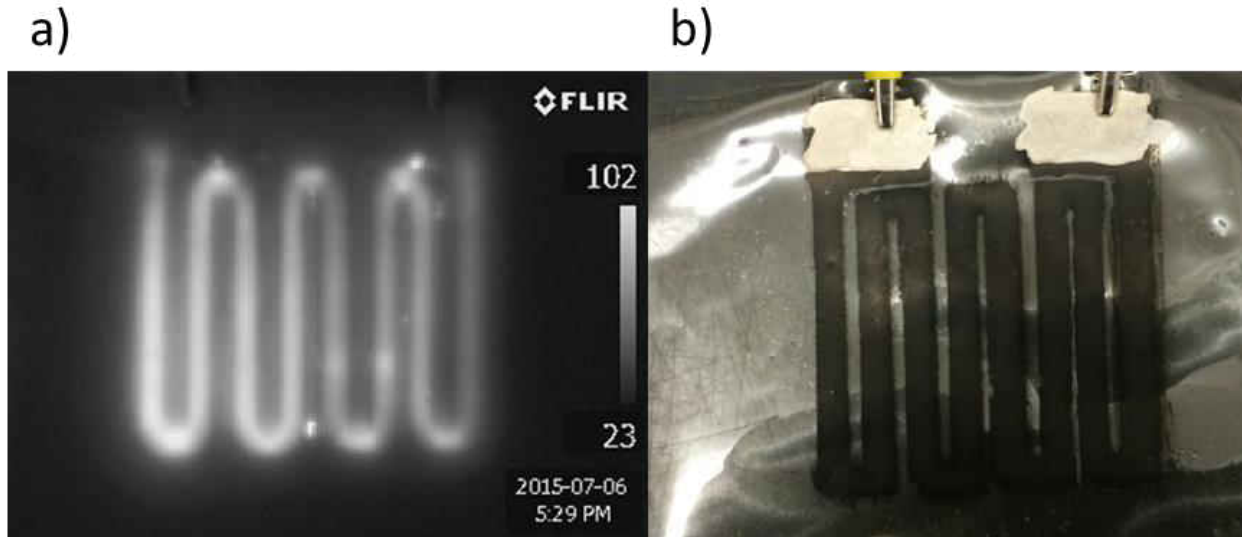


Figure 33 Thermal Heating of the SMP Thin Film using SDM Processing

The voltage was plotted against the temperature to find a trend of the heating relationship to resistivity for the SDM process. Figure 26 shows a linear relationship for temperature to voltage. This also shows that the resistance would be linear as well because of Ohm's law. Using this relationship, the maximum temperature the film can produce at any voltage is able to be found.

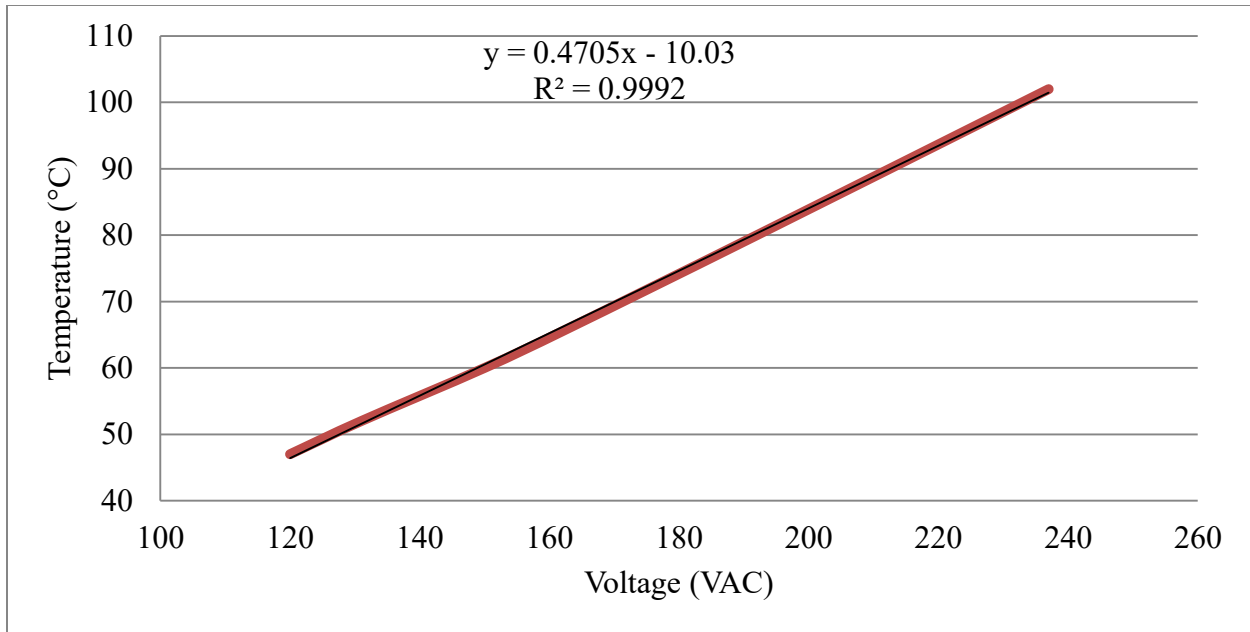


Figure 34 Temperature vs. Voltage Graph for SDM

Using Ohm's law the current values used to generate the heat of the thin film was able to be calculated. Some of the values used had some uncertainties these uncertainties are due to the values given by the equipment used. A multimeter was used to provide the voltage values that were used for joule heating of the film. The uncertainty of the values of the multimeter is ± 0.5 VAC and $\pm 0.05 \Omega$ for resistance. The thermal camera has an uncertainty of $\pm 0.5^\circ\text{C}$.

Table 4 Temperature, Voltage, and Current Measurements for SDM

Voltage (VAC)	Temperature (°C)	Current (mA)
±0.5	±0.5	±2.76*10 ⁻⁸
237	102	13.09
192	80	10.61
163	66	9.01
150	60	8.29
131	52	7.24
120	47	6.63

Table 4 above shows the voltage and temperature values that were found from the multimeter and the thermal camera. The current values were found by Ohm’s law and the resulting uncertainty is found by a systematic uncertainty analysis. The uncertainty can be found on the table above.

4.3.3 Weight Measurements

In digital processing it is imperative that all components be linear. One way to accomplish this is by characterizing the weight of the material dispersed onto the substrate. To show this material was applied to aluminum foil, which was weighed before and after to find the exact weight of the material applied. Figure 35 shows the linear trend of weight vs. speed results.

Using this trend the amount of material dispersed is able to be found which is able to be used in computer generated composites that were discussed in Chapter three.

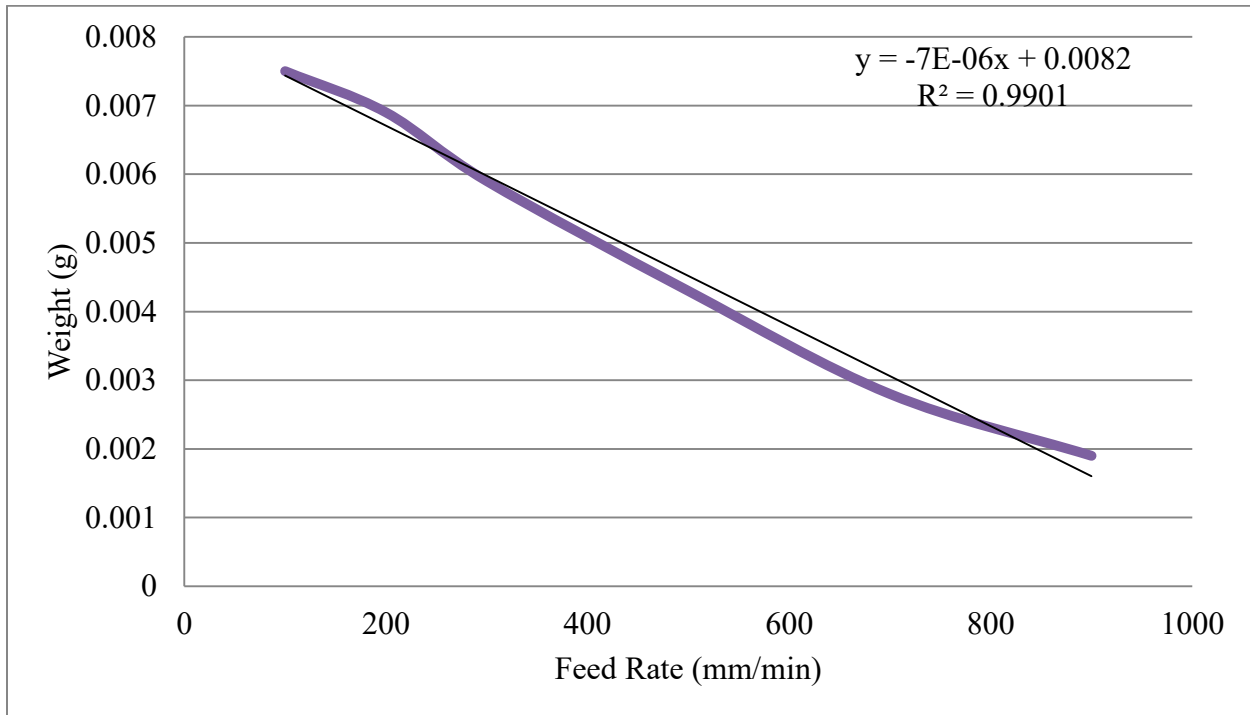


Figure 35 Lowering the Weight by Lowering the Feed Rate in SDM

Another type of weight characterization that was done on SDM processing is the weight generated by layering the material over top of each other. Figure 36 below shows as the number of layers are increased that the weight increases linearly. To find this trend 5 samples were taken at the same feed rate with different layers applied to them. This foil was then weighed before and after to find the exact weight of the material supplied.

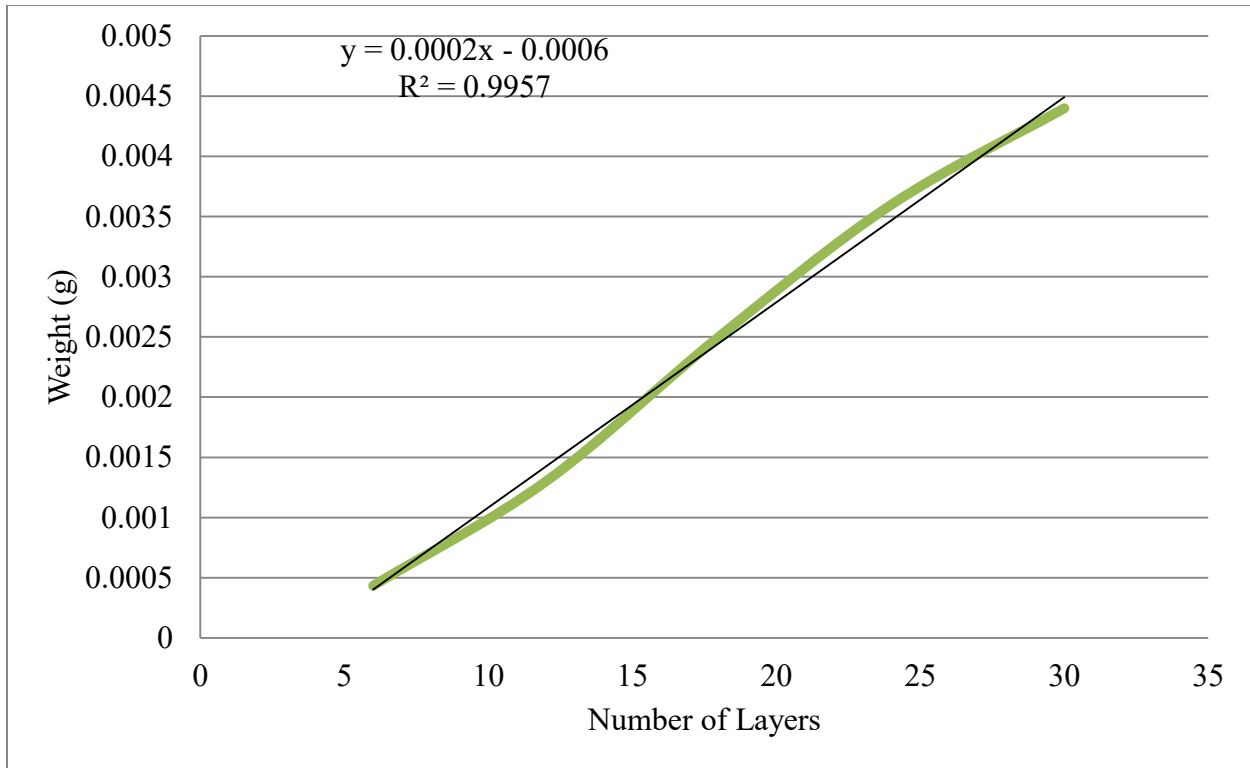


Figure 36 Increasing the Weight by Layering Using SDM

For the measurements taken for the weight distribution has 2 major uncertainties that can be contributed to some variation in the trend. One of those uncertainties is the scale that is accurate to ± 0.005 grams the other is from the spraying of the material and clogging of the nozzles. For this reason three samples were taken for all the measurements and the average of those were placed in the charts above.

4.3.4 Actuation

Shape memory polymer is a kind of smart material which can be deformed into a temporary shape and then recover to its original permanent shape through external stimuli [28]. Most SMPs have double actuation, but some are able to have triple actuation. Using SDM CNTs were applied to the SMP thin film in the form of a heater shown on Figure 33. This form was

used to distribute the heat evenly and cause the SMP to actuate uniformly. Figure 37 below shows the two shapes of the SMP the first is the original shape while the center image is the temporary shape. The permanent shape of the SMP comes from heating the SMP well above its glass transition temperature (T_g) temperature; while the temporary shape comes from deforming it by mechanical force or low thermal heat. In the figure below the temporary shape comes from slightly heating it past its T_g and then cooling it to set it.

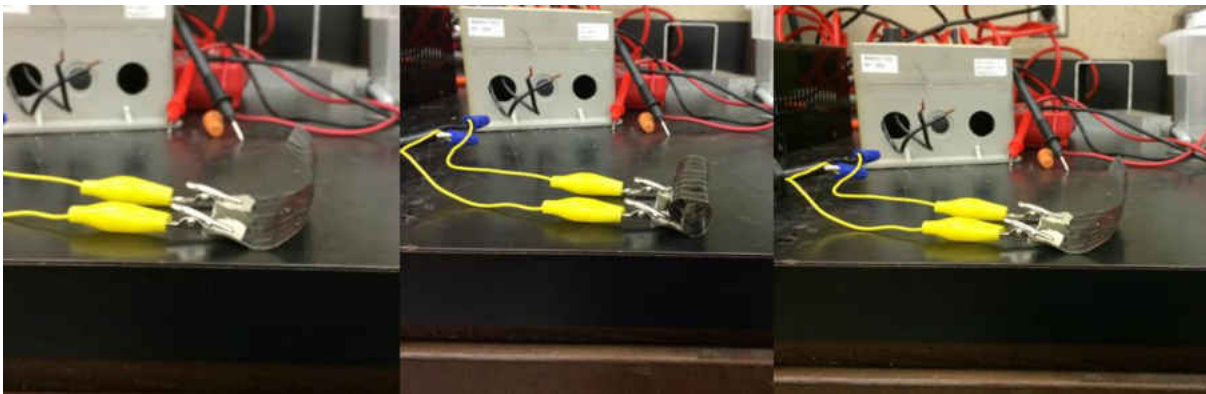


Figure 37 Actuation of the SDM Sample

The actuation occurred in the image above by applying voltage to the heater created by the SDM machine. This then caused resistive heating of the SMP which causes it to actuate back to its permanent shape. In the figure above the first and third image looks the same, but this is actually before and after actuation of the SMP. The SMP was able to recover back to its original shape with no change in its appearance.

4.4 Comparing SDM to Current Methods

As of today there are two types of systems that are similar to the SDM machine and its ability to distribute nanomaterials onto any substrate. The first is the air blast system that is

similar to the spray infiltration method, and the other is ink-jet printing carbon nano-inks which uses the same nozzle system as the SDM process. Some of the major differences between other methods are the accuracy and the controlled environment.

Air blast technique is widely used in research because of its ease to make, use and produce highly conductive CNP. One of the major differences with the Air blast technique and the SDM is the ability to image print and accuracy. While the air blast can produce highly conductive paper it is not uniform due to over spraying (which is caused when the spray hits the object and is forced into other layers), evaporation time, and its inability to digitally manufacture images accurately. SDM controls this by controlling the environment, having a nozzle that produces a solid spray pattern $235\mu\text{m}$ in size, and controlling the speed and flow rate of the material while it is producing the sample.

Ink-jet printing of CNT-inks is another common research area that has similar properties to SDM. The ink-jet printer is able to create accurate image prints and has a high resolution of 300 DPI (Dots per inch); while SDM only has a resolution of 96 DPI, but there is some differences. One major difference is that an ink-jet printer is only accurate when producing a single print while SDM can trace over the same section multiple times. Ink-jet printers are only able to print on flexible substrates like PTE (which is the most common); where SDM can print on almost any substrates including aluminum, copper, PTE, SMP, and teflon. SDM also has environmental control which allows the material to be evaporated at a faster rate than that of the ink-jet printer which could have running of the material. The final difference is length of run time. Most ink-jet printers only have a run time for less than five minutes, due to the size and shape of the sample, but SDM is able to run for longer than one and a half hours, which has been the longest run to date.

CHAPTER FIVE: CONCLUSION AND FUTURE WORK

This thesis discussed two methods of CNP fabrication and the fabrication of CNP into SMP thin films. Spray infiltration method is a versatile technique to manufacture CNP and CNP thin films, while SDM is able to control the location and distribution of the CNP. The quality and properties of the CNP thin films largely depends on the processing parameters for both major process and the resin deposition method. To ensure high quality films in the film fabrication process of the CNP, an aluminum plate was used to hold the cellulose membrane with the CNP while resin was placed on the cellulose surface. This process dissolves the cellulose membrane and replaces it with SMP resin. After the resin is sprayed it is then placed into an inferred oven at 100°C for ten minutes to dry. Controlling the oven is also important, if an infrared oven was not used the drying temperature would have to be controlled precisely to prevent wrinkling and bubbling of the films. This process is repeated one more time to ensure the DMF has dissolved all of the cellulose filter paper. Some parameters that were controlled during this process are the flow rate of the resin and the speed at which it is delivered. These parameters control the thickness of the SMP CNP produced. Dissolving of the filter paper is also controlled by those parameters. The typical thickness of SMP resin that is dispersed onto the CNP is between 2 to 10 μm depending on the speed of the belt and the flow rate of the resin.

5.1 Concluding the Spray Infiltration Process

Controlling the thickness of the spray infiltration process is the same as the resin deposition process. This is done by controlling the flow rate of the material and the speed at which the material is deposited. In Chapter four these parameters show an increase in the weight of the CNP and an increase in the thickness, both of which have an exponential decrease as the

speed of the belt is increased. Knowing this characterization the resistivity of the paper is able to be controlled. The largest thickness of the paper is around $100 \mu\text{m} \pm 2 \mu\text{m}$, with a resistivity of 14.39Ω per square, which was produced at a rate of 1 inch per minute. While the paper with the highest production rate of nine inches per minute has a resistivity of 145Ω per square and a thickness of $2 \mu\text{m}$. This highly conductive CNP film is able to be used in the heating of SMP and other enhancement of mechanical and electrical properties. Using a thermal camera the temperature values for the paper was found along with the current associated with this value. Shown in Chapter four this was a linear trend which is able to provide more information on how to determine the right voltage and current to receive the necessary temperature for actuating the SMP. Using a voltage of 25 VDC the temperatures for the CNP film ranged from 41 to 94°C with current values of 0.1 to 0.74 A. One of the most important characterizations of the spray infiltration process is the loss of material during the processing of the sample. Taking the weight of the paper and comparing it to the volume that was used to create the CNP, shows the amount of loss due to over spraying and other effects. Due to the fact that this trend is linear shows that there was a negligible loss of material because of these processing effects. The CNP created by the spray infiltration method has constant uniformity in the thickness and over the entire area; this paper is able to be used in the actuation of SMP and to enhance mechanical, electrical, and thermal properties when combined with other composites.

5.2 Concluding Spray Deposition Modeling

Spray deposition modeling is able to be used to enhance properties of a composite by controlling the material that is deposited in areas in which enhancement is needed. This also helps to lower the weight and provide products that have special abilities; such as joule heating of SMP for shape actuation. This method is able to apply most types off carbon materials like

CNTs, CNFs, HCNTs, and Graphene to any substrate such as copper, aluminum, SMP, PTE, and Teflon for the enhancement of their properties. To apply these materials to their respected substrates CNT inks were created using two different solvents one was water based and the other was ethanol based. The ethanol based ink last longer than the water based but its resistivity is much higher. The water based was used to create heater samples for the SMP to control actuation by distributing the heating over the entire area evenly. Due to the high resistivity 237 VAC was used to create the heat needed to actuate the thin film. The maximum temperature that was generated by applying this voltage was 102°C with a current of 13 mA. This was due to the resistance of the created film which was 18.1 kΩ. A trend was found by plotting the voltage versus the temperature which gave a linear trend which helps to characterize the film by being able to know the heat that is generated when any voltage is applied to the sample. Another characterization that is a major contribution to the SDM process is the weight information that is gathered by finding the weight added by layering and the weight that is distributed by increasing the federate. Both of these trends are linear, which is an advantage when characterizing a digital process by being able to control all aspects during the creation of samples. This will lead to future creations of computer controlled composites that control the material in each layer, the thickness, and the location of the deposited material.

5.3 Future Work

During the research of the spray infiltration method, SDM, and resin deposition method there were some parameters that is able to be updated or changed. For the resin deposition system increasing the flow rate would allow for faster deposition of the SMP and an increase in the dissolving of the cellulose filter paper. The spray infiltration method is able to enhance properties of a sample, but it is not a standalone film. The cellulose has to be removed by a

secondary process; if the CNP was thick enough it would separate from the filter paper by applying a shear force to the filter paper. This would make a paper that has the same ability to increase the properties of the sample without having the polyurethane film. Finally, future work for the SDM process includes improving the CNT-inks, finding the exact viscosity needed for the material for the nozzle, increasing the number of nozzles for improved quality and faster production, and the introduction of multiple arrays of nozzles for the addition of different materials in the production process. These improvements will increase the production rate, quality, and enhance of the properties.

APPENDIX A: CNC CODE

A.1 G-Code

G0 - go to G1 code

G1 - Coordinated Movement in the X and Y

G2 - Clockwise Arc

G3 - Counter Clockwise Arc

G4 - Dwell time in S<seconds> or P<milliseconds>

G28 - Home all Axis

G90 - Use Absolute Coordinates

G91 - Use Relative Coordinates

G92 - Set current position to coordinates given

A.2 M-Code

M0 - Unconditional stop - Wait for user to press a button on the LCD

M1 - Same as M0

M17 - Enable/Power all stepper motors

M18 - Disable all stepper motors; same as M84

M20 - List SD card

M21 - Initialize SD card

M22 - Release SD card

M23 - Select SD file

M24 - Start/resume SD print

M25 - Pause SD print

M26 - Set SD position in bytes

M27 - Report SD print status

M28 - Start SD write

M29 - Stop SD write

M30 - Delete file from SD

M31 - Output time since last M109 or SD card start to serial

M32 - Select file and start SD print

M42 - Change pin status via g-code

M80 - Turn on Power Supply

M81 - Turn off Power Supply

M84 - Disable steppers until next move,

M85 - Set inactivity shutdown timer with parameter S<seconds>

M92 - Set axis steps per unit

M105 - Read current temp

M106 - Fan on

M107 - Fan off

M114 - Output current position to serial port

M115 - Capabilities string

M117 - display message

M119 - Output End stop status to serial port

M140 - Set bed target temp

M190 - Wait for bed current temp to reach target temp. Waits only when heating

M201 - Set max acceleration in units/s² for print moves

M202 - Set max acceleration in units/s² for travel moves

M203 - Set maximum feed rate that your machine can sustain in mm/sec

M204 - Set default acceleration

M206 - set additional homing offset

M208 - set recover=unretract length S[positive mm surplus to the M207 S*] F[feedrate mm/sec]

M220 - set speed factor override percentage

M221 - set extrude factor override percentage

M250 - Set LCD contrast

M300 - Play beep sound

M303 - PID relay auto tune

M304 - Set bed PID parameters P I and D

M400 - Finish all moves

M500 - stores parameters in EEPROM

M501 - reads parameters from EEPROM

M502 - reverts to the default "factory settings".

M503 - print the current settings

M540 - Use S[0|1] to enable or disable the stop SD card print on end stop hit

M928 - Start SD logging

M999 - Restart after being stopped by error

A.3 A-Code

A0 - Turn nozzles OFF

A1- Nozzle 1

A2 – Nozzle 2

A3 – Nozzle 3

A4 – Nozzle 4

A5 – Nozzle 5

A6 – Nozzle 6

A7 – Nozzle 7

A8 – Nozzle 8

A9 – Nozzle 9

A10 – Nozzle10

A11 – Nozzle 11

A12 – Nozzle 12

A13 - Turn nozzles on Cycle

A14 – Purge

APPENDIX B: MATLAB CODE


```

clear all; close all; clc;

%Open File for Writing
fid = fopen('strain gauge.txt','w');
%start G-code
fprintf(fid, ';2D Printer using 12 nozzles\n');
fprintf(fid, ';Created on 2/12/2015\n\n');
fprintf(fid, 'A0\n');
fprintf(fid, 'G21; Set to mm\n');
fprintf(fid, 'G28 X0 Y0; Home Axis\n');
%fprintf(fid, 'G90; Use abs Coord\n');
fprintf(fid, 'G1\tF1300.00\n');

I = im2bw(imread('strain gauge.jpg'));
[R,C] = size(I);

N = zeros(R,12);
J = zeros(R,1);
K = zeros(1,R);
L = zeros(836,1);
M = zeros(1,836);
Iteration = 20;

for p = 1:1:Iteration
    Y = 0;
    X = 0;
    n = 4;
    temp = 1;
    check_G = 0;
    e = 1;
    f = 1;
    for i = 1:R-375
        % do foward pace
        for j = 1:C

            b = I(i,j);
            delta_x = j*0.234*2;
            n = b;

            if b == 0
                J(e) = j;
                K(e) = i;
                e = e + 1;
            end

            if n ~= temp

```

```

    if n == 0
        fprintf(fid, 'G1\tX%6.4f\n',X+delta_x);
        fprintf(fid, 'G4\n');
        L(f) = X+delta_x;
        M(f) = Y;
        f = f+1;
        for l = 1:12
            fprintf(fid, 'A%d\n',l);
        end
    end

    if n == 1
        fprintf(fid, 'G1\tX%6.4f\n',X+delta_x);
        fprintf(fid, 'G4\n');
        L(f) = X+delta_x;
        M(f) = Y;
        f = f+1;
        for l = 1:12
            fprintf(fid, 'A%d\n',l);
        end
    end
end
end
temp = n;
check_G = 0;
% Look through the image and write gcode
end
Y = Y+0.234*2;
fprintf(fid, 'G1\tY%6.4f\n',Y);
fprintf(fid, 'G4\n');
M(f) = Y;

for j = C:-1:1

    b = I(i,j);
    delta_x = j*0.234*2;
    n = b;

    if b == 0
        J(e) = j;
        K(e) = i;
        e = e + 1;
    end

    if n ~= temp
        if n == 0

```

```

        fprintf(fid, 'G1\tX%6.4f\n',X+delta_x);
        fprintf(fid, 'G4\n');
        L(f) = X+delta_x;
        M(f) = Y;
        f = f+1;
    for l = 1:12
        fprintf(fid, 'A%d\n',l);
    end
end

if n == 1
    fprintf(fid, 'G1\tX%6.4f\n',X+delta_x);
    fprintf(fid, 'G4\n');
    L(f) = X+delta_x;
    M(f) = Y;
    f = f+1;
    for l = 1:12
        fprintf(fid, 'A%d\n',l);
    end
end
end
temp = n;
check_G = 0;
% Look through the image and write gcode
end
Y = Y+0.234*2;
fprintf(fid, 'G1\tY%6.4f\n',Y);
fprintf(fid, 'G4\n');
M(f) = Y;
end
end

%end G-code
fprintf(fid, 'G4\n');
fprintf(fid, 'A0; Turn Off Nozzles\n');
fprintf(fid, 'G28 X0 Y0; Home Axis\n');
fprintf(fid, 'M84; disable motors\n');
fclose(fid);

figure;
plot(J,K,'g.');
```

```

[t,s] = size(L);

figure;
plot(L,M(1,1:t),'r.');
```

APPENDIX C: PROCESSING CODE

```

//i2c Slave Code (UNO)

#include "InkShieldLite.h"
#include "pins.h"

const byte pulsePin = 2;

int N[5] = {N0,N1,N2,N3,N4};
int I[12] = {I1,I2,I3,I4,I5,I6,I7,I8,I9,I10,I11,I12};
int P[12] = {0,0,0,0,0,0,0,0,0,0,0,0};
int Q[12] = {0,0,0,0,0,0,0,0,0,0,0,0};
int a = 0;
word R;
void spray_ink(word strip)
{
  //loop thru the strip
  for(byte i = 0; i <= 11; i++){
    if(strip & 1<<i){
      fastABCDDigitalWrite(abcdA2A5, i, HIGH); //set abcd (nozzle address)
      fastDigitalWrite(pulsePin, HIGH); delayMicroseconds(5); //pulse pin high, wait 5us
      fastDigitalWrite(pulsePin, LOW); //pulse pin low
      fastABCDDigitalWrite(abcdA2A5, i, LOW); //reset abcd
    }
  }
  //wait to be sure we don't try to fire nozzles too fast and burn them out
  delayMicroseconds(800);
}

```

```

//Set the nozzle outputs
/*
void setup_nozzle()
{
    SET_OUTPUT(N0);
    SET_OUTPUT(N1);
    SET_OUTPUT(N2);
    SET_OUTPUT(N3);
    SET_OUTPUT(N4);

    WRITE(N0,0);
    WRITE(N1,0);
    WRITE(N2,0);
    WRITE(N3,0);
    WRITE(N4,0);
}
*/
void setup_input()
{
    for(uint8_t i = 0; i < 12; i++)
    {
        pinMode(I[i],INPUT);
    }
}

void setup()
{
    //Serial.begin(9600);
    setABCDPinMode(abcdA2A5, OUTPUT); //set the abcd pins as outputs
    pinMode(pulsePin, OUTPUT); //set the pulse pin as output
    setup_input();
}

void loop()
{
    detect();
    for(int i=1;i<12;i++)
    {
        spray_ink(0x0FFF);
    }
}

```

```

void detect()
{
  for(uint8_t i = 0; i < 12; i++)
  {
    int a = digitalRead(I[i]);

    if(a == 1)
    {
      P[i] = 1;
      //Serial.println(i);
    }

    if(a == 0)
      P[i] = 0;
  }

  R = 0;
  for(uint8_t i = 0; i < 12; i++)
  {
    Q[i] = pow(P[i],i);
  }
  R = Q[1]+Q[2]+Q[3]+Q[4]+Q[5]+Q[6]+Q[7]+Q[8]+Q[9]+Q[10]+Q[11]+Q[0];
}

```

LIST OF REFERENCES

- [1] E. T. Thostenson, Z. Ren, and T. W. Chou, "Advances in the science and technology of carbon nanotubes and their composites: a review," *Composites Science and Technology*, vol. 61, 2001.
- [2] M. Ouyang, J. L. Huang, and C. M. Lieber, "Fundamental Electronic Properties and Applications of Single-Walled Carbon Nanotubes," *American Chemical Society*, vol. 35, pp. 1018-1025, 2002.
- [3] J. W. G. Wildoer, L. C. Venema, A. G. Rinzler, R. E. Smalley, and C. Dekker, "Electronic structure of atomically resolved carbon nanotubes," *Nature*, vol. 391, pp. 59-62, 1998.
- [4] T. W. Odom, J. L. Huang, P. Kim, and C. M. Lieber, "Scanning tunneling microscopy and spectroscopy studies of single wall carbon nanotubes," *Journal of Materials Research*, vol. 13, pp. 2380-2388, 1998.
- [5] T. W. Ebbesen and P. M. Ajayan, "Large-Scale Synthesis of Carbon Nanotubes," *Nature*, vol. 358, pp. 220-222, 1992.
- [6] S. N. Song, X. K. Wang, R. H. Chang, and J. B. Ketterson, "Electronic properties of graphite nanotubules from galvanomagnetic effects," *Physics Review Letters*, vol. 72, 1994.
- [7] J. P. Issi, L. Langer, J. Heremans, and C. H. Olk, "Electronic properties of carbon nanotubes: Experimental results," *Carbon*, vol. 33, pp. 941-948, 1995.
- [8] L. Langer, L. Stockman, J. P. Hermans, V. Bayot, C. H. Olk, C. V. Haesendonck, *et al.*, "Electrical resistance of a carbon nanotube bundle," *Journal of Materials Research*, vol. 9, 1994.

- [9] J. Hone, "Carbon Nanotubes: Thermal Properties," *Dekker Encyclopedia of Nanoscience and Nanotechnology*, pp. 603-610, 2004.
- [10] S. Berber, Y. K. Kwon, and D. Tomanek, "Unusually high thermal conductivity of carbon nanotubes," *Physics Review Letters*, vol. 84, pp. 4613-4616, 2000.
- [11] J. Hone, M. C. Llaguno, M. J. Biercuk, A. T. Johnson, B. Batlogg, Z. Benes, *et al.*, "Thermal properties of carbon nanotubes and nanotube-based materials," *Applied Physics A*, vol. 74, pp. 339-343, 2002.
- [12] B. I. Yakobson and P. Avouris, "Mechanical Properties of Carbon Nanotubes," *Applied Physics*, vol. 80, pp. 288-325, 2001.
- [13] V. Mokashi, D. Qian, and Y. Liu, "A study on the tensile response and fracture in carbon nanotube-based composites using molecular mechanics," *Composites Science and Technology*, vol. 67, pp. 530-540, 2007.
- [14] Y. Han and J. Elliott, "Molecular dynamics simulations of the elastic properties of polymer/carbon nanotube composites," *comput. Material Science*, vol. 39, pp. 315-323, 2007.
- [15] P. C. Ma, N. A. Siddiqui, G. Marom, and J. Kim, "Dispersion and functionalization of carbon nanotubes for polymer-based nanocomposites: A review," *Composites* vol. 41, pp. 1345-1367, 2010.
- [16] Y. Huang and E. Terenyjev, "Dispersion of Carbon Nanotubes: Mixing, Sonication, Stabilization, and Composite Properties," *Polymers*, 2012.
- [17] Q. Wang and H. Moriyama, "Carbon Nanotube-Based Thin Films: Synthesis and Properties," *Carbon Nanotubes - Synthesis, Characterization, Applications*, vol. 497-9, 2011.

- [18] Z. Wu, Z. Chen, X. Du, J. M. Logan, J. Sippel, M. Nikolou, *et al.*, "Transparent, Conductive Carbon Nanotube Films," *Science*, vol. 305, 2004.
- [19] R. Whitby, T. Fukuda, T. Maekawa, S. James, and S. Mikhailovsky, "Geometric control and tuneable pore size distribution of buckypaper and buckydiscs," *Carbon* vol. 46, 956 2008.
- [20] D. Wang, P. Song, C. Liu, W. Wu, and S. Fan, "Highly Oriented carbon nanotube papers made of aligned carbon nanotubes," *Nanotechnology*, vol. 19, p. 6, 2008.
- [21] T. H. Nama, K. Gotoa, K. Oshimab, E. V. A. Premalalb, Y. Shimamurab, Y. Inoueb, *et al.*, "Mechanical property enhancement of aligned multi-walled carbon nanotube sheets and composites through press-drawing process," *Advanced Composite Materials*, 2014.
- [22] N. Gersbenfeld, "How to Make Almost Anything," *Foreign Affairs*, vol. 91, p. 2, 2012.
- [23] S. C. Lim, D. S. Lee, K. K. Kim, Y. C. Choi, H. S. Kim, J. H. Lee, *et al.*, "Fluidic Properties of Carbon Nanotube Inks and Field Emission Properties of Ink Jet-Printed Emitters," *Japanese Journal of Applied Physics*, vol. 48, 2009.
- [24] W. Zhoul, A. B. Belay, K. Davis, and N. Sorloaica-Hickman, "Transparent Conductive Film Fabrication by Carbon Nanotube Ink Spray Coating and Ink-Jet Printing," *IEEE*, pp. 2324-2372, 2011.
- [25] R. P. Tortorich and J. W. Choi, "Inkjet Printing of Carbon Nanotubes " *Nanomaterials*, vol. 3, pp. 453-468, 2013.
- [26] J. W. Song, J. Kim, Y. H. Yoon, B. S. Choi, J. H. Kim, and C. S. Han, "Inkjet printing of single-walled carbon nanotubes and electrical characterization of the line pattern," *Nanotechnology*, vol. 19, 2008.

- [27] Z. Fan, T. Wei, G. Luo, and F. Wei, "Fabrication and characterization of multi-walled carbon nanotubes-based ink," *Journal of Materials Science*, vol. 40, pp. 5075-5077, 2005.
- [28] F. Liang, R. Sivilli, J. Gou, Y. Xu, and B. Mabbot, "Electrical actuation and shape recovery control of shape-memory polymer nanocomposites," *International Journal of Smart and Nano Materials*, vol. 4, pp. 167-178, 2013.